Time-Dependent Models of Signal Transduction Networks

by

Jonathan Trinity Young

A Dissertation Presented in Partial Fulfillment
of the Requirement for the Degree
Doctor of Philosophy

Approved November 2013 by the
Graduate Supervisory Committee:

Dieter Armbruster, Chair
Rodrigo Platte
John Nagy
Steven Baer
Jesse Taylor

ARIZONA STATE UNIVERSITY

December 2013

ABSTRACT

Signaling cascades transduce signals received on the cell membrane to the nucleus. While noise filtering, ultra-sensitive switches, and signal amplification have all been shown to be features of such signaling cascades, it is not understood why cascades typically show three or four layers. Using singular perturbation theory, Michaelis-Menten type equations are derived for open enzymatic systems. When these equations are organized into a cascade, it is demonstrated that the output signal as a function of time becomes sigmoidal with the addition of more layers. Furthermore, it is shown that the activation time will speed up to a point, after which more layers become superfluous. It is shown that three layers create a reliable sigmoidal response progress curve from a wide variety of time-dependent signaling inputs arriving at the cell membrane, suggesting that natural selection may have favored signaling cascades as a parsimonious solution to the problem of generating switch-like behavior in a noisy environment.

DEDICATION

This work is dedicated to my family, friends, mentors, and colleagues. Without your support this research would not have been possible.

ACKNOWLEDGEMENTS

I would like to acknowledge Professor Amrbruster and Professor Nagy for introducing me to the research topic and for numerous useful discussions over the past several years. I would like to acknowledge my committee members Professor Taylor, Professor Platte, and Professor Baer for useful feedback. I would like to thank my friends and colleagues Juan Renova, Tacker Frink, Ben Trey, and Hao Liu for helpfully proofreading drafts of my documents. Also, this work was partially supported by More Graduate Education at Mountain States Alliance (MGE@MSA), Alliance for Graduate Education and the Professoriate (AGEP), National Science Foundation (NSF) Cooperative Agreement No. HRD-0450137 and by the Volkswagen Foundation under the program on Complex Networks.

TABLE OF CONTENTS

LIST OF FIGURES

Chapter 1

BACKGROUND

1.1 Motivation

The goal of this research is to use mathematical tools and systems theory to further understand why certain biochemical networks have evolved the way they have. Over the past century, scientists have meticulously catalogued the various chemical species that compose a living cell. However, it is still not fully understood how these molecules interact to create life. The advent of high-throughput experiments to collect large, genomic datasets together with more refined experiments have enabled scientists to diagram which molecules interact with each other, but there are still many holes left to be filled, and many open questions about quantitative values and the purpose of certain recurring network structures.

In particular, there are certain motifs in the signaling networks of eukaryotic organisms that are highly conserved. Understanding how these pathways operate will not only elucidate the inner workings of the cell, but could also be used to develop treatments for diseases. For example, it has been found that the Ras-Raf-MEK-ERK pathway is constitutively active in many forms of cancer. It is possible that therapies which target that pathway could provide an effective treatment [1].

Various mathematical tools for understanding systems of interacting components have been developed for a wide variety of different disciplines, and they have been fruitful when applied to cell biology. The use of applied mathematics to study enzyme kinetics has been around for over a century. In 1913, Michaelis and Menten wrote a seminal paper establishing the framework for the study of enzyme kinetics and

introduced a simplified model in which steady-state parameters could be easily derived experimentally. Over the years, numerous attempts to validate the Michaelis-Menten model with mathematical rigor have been made, but it was not until a paper by Segel and Slemrod in 1989 that the most accepted scaling of the system and error bounds were introduced. In 1996 Borghans *et al.* used a change of variables to refine the Segel and Slemrod work and improved the range of validity. This framework is based on the total quasi-steady state assumption (tQSSA) and has been used to study more complicated enzymatic reaction networks. One such study in 2007 by Gomez-Uribe *et al.* introduced a time-dependent flux of enzymes into a common signaling cycle motif in an effort to study the module's filtering characteristics, and they appealed to the tQSSA to obtain a simplified model that was easier to deal with. However, few attempts have been made to study rigorously how the introduction of a time-dependent term could affect the validity of the approximate model. For example, one assumption of the tQSSA is that there is a brief transient period of complex formation, but it can be shown that the transient can be extended depending on the flux term. This work tries to address this issue and also demonstrates how a non-autonomous model could be used modularly by applying it to simple signaling cascades.

1.2 Derivation of Mass-Action Model

There are many ways to model the behavior of molecular reactions. One approach based on first-principle arguments treats each atom as a quantum mechanical object and then tries to find a solution to Schrödinger's Equation [2]. However, even after numerous approximating assumptions are made to make the numerics easier, this problem is not very tractable even when supercomputers are employed. For the most part, the behavior of the cell is dictated by the number of molecules present and their location. Thus, knowledge of the geometry of each molecule can be sacrificed *in lieu*

of a model that is easier to deal with. In this vein, a stochastic differential equation is one of the more detailed models. It encapsulates the stochastic nature of the reactive events and diffusive movements. If it is assumed that the molecules diffuse rapidly enough in a constant volume and temperature medium, then the spatial aspects can be neglected. The system can be entirely described by an n dimensional vector over the non-negative integers where the i^{th} component of the vector corresponds to the number of molecules of the i^{th} type.

The Chemical Master Equation (CME) is a set of ordinary differential equations (ODEs) that describe the probability distribution of each possible state over time. Higham gives a good review of how, starting from the Chemical Master Equation, the mass-action model of biochemical kinetics is derived [3]. The CME can be stated as:

$$\frac{dP(x,t)}{dt} = \sum_{j=1}^{M} (a_j(x-\nu_j)P(x-\nu_j,t) - a_j(x)P(x,t))$$

where $P(x,t)$ is the probability that the system will be in state x at time t, M is the number of reactions, ν_j is an integer vector that represents the reaction that takes the state x to $x-\nu_j$, and $a_j(x-\nu_j)$ is the propensity for the j^{th} reaction to occur. Since the number of possible states that the system can be in is usually too large to deal with, the CME is not useful to deal with directly.

In 1976 and 1977, Dan Gillespie wrote a pair of papers in which he detailed a Stochastic Simulation Algorithm (SSA), which uses a kinetic Monte Carlo method to compute sample paths the system state could take instead of computing the entire probability distribution [4, 5]. By computing many sample paths, statistics such as the mean and variance can be numerically estimated. Modifications to speed up the algorithm have been suggested; however, simulating a large number of molecules undergoing numerous reactions can still be computationally expensive [6]. The Tau-Leaping Method is a scheme that approximates an SSA sample path by assuming that

the propensity functions remain constant during a fixed time interval τ [7]. Then the number of reactions for each type can be counted in the time interval τ and the system can be updated more rapidly than going one reaction at a time. Whereas the SSA pulls from exponential distributions, the Tau Leaping method uses Poisson distributions with means $a_j(X(t))\tau$ where $X(t)$ is the system's current state.

If it is assumed that the propensity functions are large, then the Poisson random variables can be well-approximated by normal random variables. This gives rise to a discrete time recurrence relation over the reals, and by allowing $\tau \to 0$, a stochastic ODE known as the Chemical Langevin Equation (CLE) is derived [8]. If the approximated state is given as Y, which is an n dimensional vector over the reals, then the equation can be stated as

$$dY(t) = \sum_{j=1}^{M} \nu_j a_j(Y(t))dt + \sum_{j=1}^{M} \nu_j \sqrt{a_j(Y(t))} dW_j(t),$$

where the W_j's are independent scalar Brownian motions. The CLE can be thought of as having both a stochastic part and a deterministic part. If the system size increases, but the concentrations of the molecules remain the same, then the deterministic part will dominate. By ignoring the stochastic portion, a set of ODEs emerge. The resulting set of ODEs is the most studied model of molecular reactions. Typically, the derivation of the ODEs is done in an *ad hoc* way by appealing to the law of mass-action, which states that the rate at which a reaction occurs is proportional to the concentrations of each reactant involved. Hence, the set of ODEs derived from the CLE is sometimes referred to as the mass-action model.

Though the intuitive mass-action argument and the formal derivation reach the same conclusion, the formal derivation specifies the conditions in which the mass-action should be applied. One condition is that the number of molecules involved should be large enough such that stochastic nature of individual molecular reactions

get averaged out. There has been some arguments as to whether this condition is satisfied in a molecular environment [9, 10]. In certain cases, such as modeling a small number of transcription factors binding to a DNA strand, the ODE model might not work as well as a more refined model. In other cases, such as modeling a metabolic network, the ODE model may suffice. Finding a way to connect the varying scales in the cellular environment is still an open problem. Another condition that must be satisfied is that the system be spatially homogenous. In the cell where the space can be highly compartmentalized, this assumption does not always hold. One work-around is to label the same molecule in different compartments as different chemical species and then add a flux term between the two compartments in the mass-action model. Even though there have been discussions as to whether the mass-action accurately portrays cellular behavior, it serves as a good starting point in which more refined models can be compared [9, 10, 3].

1.3 Derivation of Michaelis-Menten Equation

One of the most basic chemical reactions studied is the enzyme-substrate reaction. Early in the 20th century, the mechanism in which an enzyme converted a substrate into a product molecule was not fully understood. In 1913, Leonor Michaelis and Maud Menten proposed a mass-action model where the enzyme binds to the substrate to form an intermediate complex molecule [11, 12]. The complex can then either disassociate back into an enzyme and substrate, or the enzyme can successfully catalyze the conversion of substrate to product. The representative stoichiometry would be

$$E + S \underset{d_1}{\overset{a_1}{\rightleftarrows}} C \xrightarrow{k_1} E + P,$$

where a_1, d_1, and k_1 are rate constants. The corresponding system of equations is

$$\dot{E} = -a_1 ES + (d_1 + k_1)C, \tag{1.1a}$$

$$\dot{S} = -a_1 ES + d_1 C, \tag{1.1b}$$

$$\dot{C} = a_1 ES - (d_1 + k_1)C, \tag{1.1c}$$

$$\dot{P} = k_1 C, \tag{1.1d}$$

$$E(0) = E_0, \quad S(0) = S_0, \quad C(0) = P(0) = 0 \tag{1.1e}$$

where the initial conditions represent the case where there is an initial concentration of enzymes and substrates, but no reaction has yet occurred. From a physical sense, since no molecules are added or destroyed from the system, and also by examining (1.1), it is clear that certain quantities are conserved. Hence, (1.1) is equivalent to a system of two ODEs and two algebraic equations.

$$E = E_0 - C, \tag{1.2a}$$

$$P = S_0 - (S + C), \tag{1.2b}$$

$$\dot{S} = -a_1(E_0 - C)S + d_1 C, \tag{1.2c}$$

$$\dot{C} = a_1(E_0 - C)S - (d_1 + k_1)C, \tag{1.2d}$$

$$S(0) = S_0, \quad C(0) = 0. \tag{1.2e}$$

Michaelis and Menten also proposed a method in which (1.2) can be approximated by a one dimensional ODE. In 1925, G.E. Briggs and J.B.S Haldane refined that approach and proposed the following: suppose that the complex does not change much during the time-scale of the substrate depletion [13]. This can be achieved if the number of enzymes are much larger than the number of substrates since any free enzyme will quickly bind to a free substrate. After a quick transient period in which the substrate concentration has not decayed much, $\dot{C} \approx 0$. This is known as the

standard quasi-steady state assumption (sQSSA). If $\dot{C} = 0$, then C can be solved for in (1.2d).

$$C = \frac{E_0 S}{K_m + S}, \tag{1.3}$$

where $K_m = \frac{d_1 + k_1}{a_1}$ is the Michaelis-Menten constant. Then (1.3) can be substituted in (1.2c) to get that

$$\dot{S} = \frac{-V_{max} S}{K_m + S}, \quad S(0) = S_0, \tag{1.4}$$

where $V_{max} = k_1 E_0$ is the maximal possible rate at which the product could be formed. K_m can also be regarded as the substrate concentration at which the formation rate of the product is half of V_{max}. The initial condition in (1.4) assumes that the substrate has not decayed noticeably during the initial transient period. Equation (1.4) is generally referred to as the Michaelis-Menten equation. In [14, 15] it was shown that (1.4) has a closed form solution.

$$S(t) = K_m W \left[\frac{S_0}{K_m} \exp\left(\frac{S_0}{K_m} - \frac{V_{max} t}{K_m} \right) \right],$$

where W is the Lambert-W function. Experimentally, it easier to obtain the parameters K_m and V_{max} than it is to obtain the reaction rate constants, and it is easier to find the steady-state parameters in literature rather than the dynamic parameters.

1.4 Enzymatic and Signaling Cascades

In general, an enzymatic cascade is a sequence of chemical reactions in which the product of one reaction serves as the enzyme in the next reaction downstream. Enzymatic cascades are important structures in blood coagulation models. In 1964, Davie and Ratnoff [16] and Macfarlane [17] independently proposed a waterfall sequence which enables a small signal to become amplified such that a large number of fibrin molecules can be created to form a blood clot. Then in 1966, Levine studied the enzyme amplifier kinetics by constructing a time-dependent mathematical model

[18]. This model neglected any feedback and looked at just a sequence of linear reactions. A unit pulse was introduced at the first stage and this signal proliferated for n stages. The gain of the system was defined as the ratio of the steady state of the n^{th}-layer versus the steady state value of the initial layer. Also, the temporal dynamics of a 3-layered system was investigated by varying the duration of the unit pulse. The mathematical model of [18] corroborated the amplification scheme and also discovered sensitivities to the reaction rates.

Other types of important cascades are signaling cascades. In a signaling cascade, information in the form of a chemical cue received at the cell membrane is proliferated to transcription factors via a sequence of chemical reactions. Of particular importance to eukaryotic cells are mitogen activated protein kinase (MAPK) cascades which are involved in numerous cellular processes such as differentiation, apoptosis, and carcinogenesis [19, 20, 1]. Since signaling cascades play important roles in certain types of cancer cells, understanding these cascades could lead to novel therapies [1]. One important trait of MAP kinase cascades is that they typically have 3 or 4 layers [19]. However, it is still not entirely understood why a 3 or 4-layered cascade should be evolutionarily conserved.

In eukaryotes, there is an important and highly conserved component in signaling pathways, a family of proteins that compose the MAPK cascade. This module is a cascade of chemical reactions where the activated form of one protein serves as an enzyme to activate a protein downstream. Typically, there are three to four levels in a MAPK cascade [19].

In 1996, Huang and Ferrell constructed a mathematical model to study the dynamics of a 3-layered MAP kinase cascade with double phosphorylation cycles [21]. They designed a mass-action differential model for the closed system diagrammed in Figure 1.1. The initial concentration of the input was taken as the stimulus and the

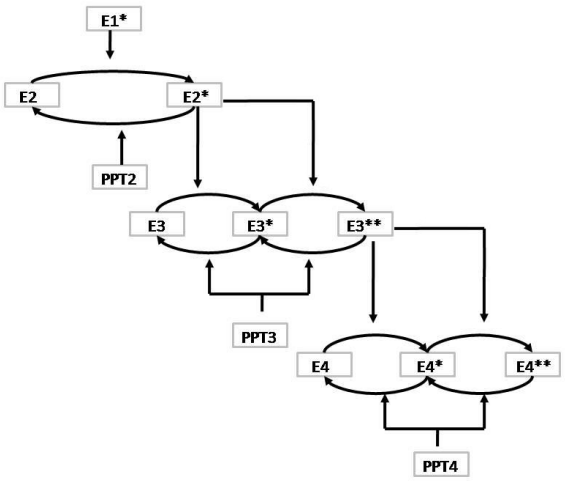

Figure 1.1: Huang and Ferrell Model

steady-state concentration of the output was regarded as the response. They discovered that the multiple layers help create an ultrasensitive signal-to-response curve. This switch-like, ultra-sensitivity was first described by Goldbeter and Koshland in 1984 [22]. The cascade behaves like a cooperative enzyme with a steeper sigmoidal signal-to-response curve than one sees with a traditional Michaelis-Menten reaction. This behavior is ideal for biological mechanisms requiring a switch-like response. Qiao *et al.* expanded on the work of [21] in 2007 by exploring from a wider range of parameters to see if other types of signal-to-response curves were possible [23]. They discovered the existence of bistability and oscillations in the Huang and Ferrell model.

In 2007, Gomez-Uribe *et al.* analyzed the operating regimes of a single cycle of covalent modification, one of the important components in a signaling cascade [24]. They discovered that a single cycle can exhibit 4 steady-state response regimes. By appealing to the total quasi-steady-state assumption [25], they were able to reduce their mass-action system into a single ordinary differential equation for the activated protein. They use this approximated model to study the dynamic response with respect to sinusoidal input. They find that a single cycle acts as a low-pass filter.

This makes the cycle of covalent modification ideal to filter out high frequency noise.

In 2007, Ventura *et al.* looked at a simplified version of a signaling cascade. Their model is essentially the closed system of Figure 2.12. Using the quasi-steady state assumption, they were able to derive a one parameter equation for each module of a cycle of covalent modification. They then model a signaling cascade by linking together these one parameter modules. They discover damped oscillations in the first unit of a ten unit chain in both the mass-action description of Figure 2.12 and their approximation model. They also consider the case where the system is in a steady-state and one of the parameters is perturbed. This information gets propagated in both directions of the chain, which suggests that multiple layers in the cascade structure can facilitate cross-talk between networks without the need of explicit feedback loops.

1.5 Perturbation Analysis of Michaelis-Menten Equations

Since Equation (1.4) is an approximation, it is important to investigate is the error in using it. One approach to answer this question has been to use singular perturbation theory. References [26, 27] are excellent texts describing perturbation methods and applications. One approach to this problem is to first scale Equation (1.2) and then identify a small parameter. However, early authors scaled C by E_0 and S by S_0 and set their small parameter as $\epsilon = E_0/S_0$ [27, 28]. However, in 1989, Segel and Slemrod gave a more rigorous derivation and scaling of the system [29].

They introduce the following scales for Equation (1.2):

$$s = \frac{S}{S_0},$$
$$c = \frac{C}{\bar{C}},$$
$$\tau = \frac{t}{t_C},$$
$$T = \frac{t}{t_S},$$

where $\bar{C}$ is an estimate of the maximal complex concentration, t_C is an estimate for the fast time scale, and t_S is an estimate for the slow time scale. It is assumed that in the initial transient period, the substrate depletion is minimal and $S \approx S_0$. By substituting S_0 for S in (1.2d), the authors were able to derive the following for C:

$$C(t) = \bar{C}[1 - \exp(-kt)], \tag{1.5}$$

where

$$\bar{C} = \frac{E_0 S_0}{K_m + S_0}, \tag{1.6}$$
$$k = a_1(S_0 + K_m).$$

They used (1.5) to get an estimate for the fast time scale.

$$t_C = k^{-1}. \tag{1.7}$$

The characterization of a time scale from [27] is used to estimate the slow time scale as follows:

$$t_S = (S_{max} - S_{min}) / \left| \frac{dS}{dt} \right|_{max}. \tag{1.8}$$

They estimate t_s by plugging S_0 into (1.4) to obtain:

$$t_S = \frac{K_m + S_0}{k_1 E_0}. \tag{1.9}$$

The authors obtained the following dimensionless parameters:

$$\sigma = \frac{S_0}{K_m}, \quad \kappa = \frac{d_1}{k_1}, \quad \epsilon = \frac{E_0}{K_m + S_0}.$$

In the fast time scale, the governing equations for (1.2) are:

$$\begin{aligned} s'(\tau) &= \epsilon \left[-s + \frac{\sigma}{\sigma+1} cs + \frac{\kappa}{(\kappa+1)(\sigma+1)} c \right], \\ c'(\tau) &= s - \frac{\sigma}{\sigma+1} cs - \frac{1}{\sigma+1} c, \\ s(0) &= 1, \quad c(0) = 0. \end{aligned} \tag{1.10}$$

Assuming that

$$s(\tau) \sim s^{(0)}(\tau) + \epsilon s^{(1)}(\tau) + \cdots, \quad c(\tau) \sim c^{(0)}(\tau) + \epsilon c^{(1)}(\tau) + \cdots,$$

then the $O(1)$ solutions for (1.10) are:

$$s^{(0)}(\tau) = 1, \quad c^{(0)}(\tau) = 1 - e^{-\tau}. \tag{1.11}$$

In the slow time scale, the governing equations are:

$$\begin{aligned} s'(T) &= (\kappa+1)(\sigma+1) \left[-s + \frac{\sigma}{\sigma+1} cs + \frac{\kappa}{(\kappa+1)(\sigma+1)} c \right], \\ \epsilon c'(T) &= (\kappa+1)(\sigma+1) \left[s - \frac{\sigma}{\sigma+1} cs - \frac{1}{\sigma+1} c \right]. \end{aligned} \tag{1.12}$$

Again, assuming that

$$s(T) \sim s_0(T) + \epsilon s_1(T) + \cdots, \quad c(T) \sim c_0(T) + \epsilon c_1(T) + \cdots, \tag{1.13}$$

then the governing equations for (1.12) become:

$$\begin{aligned}
s_0'(T) + \epsilon s_1'(T) + \cdots = {} & (\kappa+1)(\sigma+1)\left[-s_0 + \frac{\sigma}{\sigma+1}c_0 s_0 + \frac{\kappa}{(\kappa+1)(\sigma+1)}c_0\right] \\
& + \epsilon(\kappa+1)(\sigma+1)\left[-s_1 + \frac{\sigma}{\sigma+1}(c_0 s_1 + c_1 s_0) + \frac{\kappa}{(\kappa+1)(\sigma+1)}c_1\right] \\
& + O(\epsilon^2), \\
0 + \epsilon c_0'(T) + \cdots = {} & (\kappa+1)(\sigma+1)\left[s_0 - \frac{\sigma}{\sigma+1}c_0 s_0 - \frac{1}{\sigma+1}c_0\right] \\
& + \epsilon(\kappa+1)(\sigma+1)\left[s_1 - \frac{\sigma}{\sigma+1}(c_0 s_1 + c_1 s_0) - \frac{1}{\sigma+1}c_1\right] \\
& + O(\epsilon^2).
\end{aligned}$$

The $O(1)$ equations become

$$c_0(T) = \frac{(\sigma+1)s_0}{\sigma s_0 + 1}, \quad s_0'(T) = -c_0, \tag{1.14}$$

which are identical to the Michaelis-Menten equations when scaled back to the original variables. The $O(\epsilon)$ equations are found to be:

$$c_1(T) = \frac{s_1(1+\sigma)}{(1+\sigma s_0)^2} + \frac{(\sigma+1)^2 s_0}{(1+\kappa)(\sigma s_0+1)^4}, \tag{1.15a}$$

$$s_1'(T) = -c_1 - c_0' = -p(T)s_1 + q(T), \tag{1.15b}$$

where

$$p(T) = \frac{1+\sigma}{(1+\sigma s_0)^2}, \quad q(T) = \frac{(\sigma+1)^2 s_0}{(\sigma s_0+1)^3}\left(1 - \frac{1}{(1+\kappa)(\sigma s_0+1)}\right). \tag{1.16}$$

Segel and Slemrod use the $O(\epsilon)$ equations to determine the range of validity of their model. If the magnitudes of s_1 and c_1 are much larger than one, then the errors could be large when using the first order approximation.

In 1996, Borghans used a change of variables to extend the sQSSA [25]. If $S_c =$

$S + C$, then an equivalent differential model for (1.2) is:

$$\dot{S}_c = -k_1 C, \tag{1.17a}$$

$$\dot{C} = a_1(E_0 - C)(S_c - C) - (d_1 + k_1)C, \tag{1.17b}$$

$$S_c(0) = S_0, \quad C(0) = 0. \tag{1.17c}$$

The total quasi-steady state assumption states that Equation (1.17b) is approximately equal to zero on the timescale of the total substrate depletion. By assuming $\dot{C} = 0$, then the following quadratic equation is derived for C:

$$C^2 - (E_0 + K_m + S_c)C + E_0 S_c = 0. \tag{1.18}$$

The first Padé approximant to (1.18) is:

$$C = \frac{E_0 S_c}{E_0 + K_m + S_c}. \tag{1.19}$$

By substituting (1.19) into (1.17a) one obtains:

$$\dot{S}_c = \frac{-V_{max} S_c}{E_0 + K_m + S_c}. \tag{1.20}$$

By using a similar argument as used in [29], Borghans derived the following slow timescale:

$$t_{sc} = \frac{E_0 + S_0 + K_m}{k_1 E_0}, \tag{1.21}$$

and the following condition for the approximation to be valid is:

$$\epsilon = \frac{k_1 E_0}{a_1(E_0 + S_0 + K_m)} \ll 1. \tag{1.22}$$

Equivalent conditions to (1.22) are:

$$\frac{k_1}{a_1} \ll E_0 + S_0,$$

$$k_1 \ll d_1,$$

$$E_0 \ll S_0 + K_m.$$

So if the sQSSA is valid, then so too is the tQSSA. However, the tQSSA greatly extends the regime of validity.

In 2007, Gomez-Uribe *et al.* use the tQSSA to study the operating regimes of a cycle of covalent modification motif, such as seen in the phosphorylation and dephosphorylation cycle in a MAPK cascade [24]:

$$\begin{aligned} E_1 + S &\underset{d_1}{\overset{a_1}{\rightleftarrows}} C_1 \xrightarrow{k_1} E_1 + P, \\ E_2 + P &\underset{d_2}{\overset{a_2}{\rightleftarrows}} C_2 \xrightarrow{k_1} E_2 + S. \end{aligned} \tag{1.23}$$

By applying the tQSSA, the authors derived the following approximation for (1.23):

$$\dot{P}_c = k_1 \frac{\bar{E}_1(\bar{S} - P_c(t))}{K_{m1} + \bar{E}_1 + \bar{S} - P_c(t)} - k_2 \frac{\bar{E}_2 P_c(t)}{K_{m2} + \bar{E}_2 + P_c(t)}, \tag{1.24}$$

where

$$P + C_2 = P_c, \quad S + C_1 + P + C_2 = \bar{S}, \quad E_1 + C_1 = \bar{E}_1, \quad E_2 + C_2 = \bar{E}_2,$$

and

$$K_{m1} = \frac{k_1 + d_1}{a_1}, \quad K_{m2} = \frac{k_2 + d_2}{a_2}.$$

The authors used (1.24) to discover four different steady-state regimes. In addition, they investigated the dynamic response of (1.23) by allowing $\bar{E}_1$ to be dependent on time. To study the filtering characteristics of their model, they set

$$\bar{E}_1(t) = E_0(1 + a\sin(\omega t)) \tag{1.25}$$

in model (1.24). They discovered that the covalent modification cycle acts as a low-pass filter. However, the authors do not provide a rigorous perturbation analysis of the time-dependent model.

Chapter 2

TIME-DEPENDENT MODELS OF ENZYMATIC AND SIGNAL TRANSDUCTION CASCADES

2.1 Basic Model of an Enzymatic Cascade

The simplest enzymatic cascade would have the chemical network in Figure 2.1. The enzymes at the top layer flow into the system at a rate of $\bar{\lambda}(t)$. However, to keep

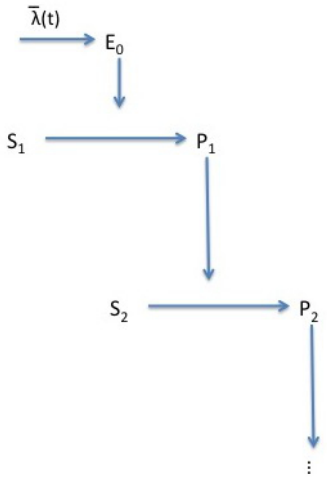

Figure 2.1: A basic enzymatic cascade.

the model as general as possible, $\bar{\lambda}$ could possibly be negative, which represents the enzymes flowing into and out of the system with a rate that is independent of the number of enzymes in the system. As an example, suppose there are ligands binding to a membrane receptor and they flow across in a periodic fashion. Then the receptor will be activated and deactivated in a similar way. These initial enzymes then convert a substrate into a product. The product then acts as an enzyme to convert a different substrate downstream and so forth. To analyze the basic structure of the cascade, it

will be assumed that no intermediate complexes are formed. Then an n-stage cascade would have the following stoichiometry:

$$\begin{aligned}
\varnothing &\xrightarrow{\bar{\lambda}(t)} E, \\
E + S_1 &\xrightarrow{a_1} E + P_1, \\
P_1 + S_2 &\xrightarrow{a_2} P_1 + P_2, \\
&\vdots \\
P_{n-1} + S_n &\xrightarrow{a_n} P_{n-1} + P_n.
\end{aligned}$$

The corresponding set of mass-action equations is:

$$\begin{aligned}
\dot{E} &= \bar{\lambda}(t), \\
\dot{S}_1 &= -a_1 E S_1, \\
\dot{P}_1 &= a_1 E S_1, \\
\dot{S}_2 &= -a_2 P_1 S_2, \\
\dot{P}_2 &= a_2 P_1 S_2, \\
&\vdots \\
\dot{S}_n &= -a_n P_{n-1} S_n, \\
\dot{P}_n &= a_n P_{n-1} S_n, \\
E(0) = P_i(0) &= 0, \quad S(0) = \bar{S}_i, \quad \text{for } 1 \leq i \leq n.
\end{aligned} \tag{2.1}$$

To analyze system (2.1), it will be prudent to express each module as an input/output operator. The basic module:

$$\begin{aligned}
\varnothing &\xrightarrow{\bar{\lambda}(t)} E, \\
E + S &\xrightarrow{a_1} E + P,
\end{aligned}$$

has the corresponding set of equations:

$$\begin{aligned} \dot{E} &= \bar{\lambda}(t), \\ \dot{S} &= -a_1 ES, \\ \dot{P} &= a_1 ES, \\ E(0) = P(0) = 0, &\quad S(0) = \bar{S}. \end{aligned} \tag{2.2}$$

Mass conservation and scaling will be used to simplify and non-dimensionalize system (2.2). Clearly, $S(t)+P(t) = \bar{S}$. Hence, system (2.2) can be reduced to one dimension. Also, E can be solved for explicitly.

$$\begin{aligned} E &= \int_0^t \bar{\lambda}(x)dx =: \bar{\Lambda}(t) \\ P &= \bar{S} - S \\ \dot{S} &= -a_1 \bar{\Lambda} S \\ S(0) &= \bar{S}. \end{aligned} \tag{2.3}$$

It can be assumed that there cannot ever be an infinite enzyme concentration, so $\bar{\Lambda}$ should have a supremum:

$$\sup_{t\in[0,\infty)} \{\bar{\Lambda}(t)\} = \bar{E} < \infty.$$

To scale the system, the time-scale as characterized in [27] will be used to estimate the time-scale that S operates on. For general $\bar{\lambda}$,

$$\frac{S_{max} - S_{min}}{\left|\dot{S}\right|_{max}} \approx \frac{1}{a_1 \bar{E}} =: t_S.$$

This estimate can be improved with more information about $\bar{\lambda}$. The variables in system (2.3) can be scaled as:

$$T = \frac{t}{t_S}, \quad s(T) = \frac{S(t)}{\bar{S}}, \quad p(T) = \frac{P(t)}{\bar{S}}, \quad \Lambda(T) = \frac{\bar{\Lambda}(t)}{\bar{E}}.$$

Then the scaled version of system (2.3) is:

$$\begin{aligned}
\Lambda(T) &= \frac{1}{\bar{E}} \int_0^{t_s T} \bar{\lambda}(x)dx \\
p(T) &= 1 - s(T), \\
s'(T) &= -\Lambda s, \\
s(0) &= 1.
\end{aligned} \tag{2.4}$$

The system (2.4) has an explicit solution:

$$s(T) = \exp\left(-\int_0^T \Lambda(x)dx\right), \quad p(T) = 1 - \exp\left(-\int_0^T \Lambda(x)dx\right). \tag{2.5}$$

A cascade with identical modules can be modeled as a functional operator. First, it will be useful to fully describe the function space that the operator acts on. To make the model physically relevant, Λ, which represents the total, scaled concentration of enzymes in the system, should be bounded, continuous, and non-negative. If the enzymes are pumped into the system with no mechanism to escape or if the enzymes flow into and out of the system in a periodic fashion forever, then the integral of Λ over time will be infinite. It can also be assumed that the enzymes are introduced into the system, so none are initially present. Finally, if Λ is initially zero for a period of time, then nothing will happen in the system. So it can be assumed that Λ is positive in a neighborhood about zero. To summarize, there exists a $\delta_0 > 0$ such that

$$\begin{aligned}
&\Lambda(T) \in C^0([0,\infty)), \\
&\Lambda(T) \geq 0, \\
&\sup_{[0,\infty)} \{\Lambda(T)\} = 1, \\
&\Lambda(0) = 0, \\
&\Lambda(T) > 0 \text{ for all } 0 < T \leq \delta_0, \\
&\int_0^\infty \Lambda(x)dx = \infty.
\end{aligned} \tag{2.6}$$

Let Λ_{set} be the set of functions from $[0, \infty)$ to $[0, 1]$ that satisfy the properties in (2.6). Let

$$F : \Lambda_{set} \to \Lambda_{set},$$

be defined as:

$$F(\Lambda)(T) = 1 - \exp\left(-\int_0^T \Lambda(x)dx\right). \tag{2.7}$$

By the properties of the exponential function, it is straightforward to show that F is well-defined. Then the output for an n-stage cascade can be computed as:

$$p_n(T) = F^n(\Lambda)(T).$$

For simplicity, the dependence on T will be assumed. Hence,

$$p_n = F^n(\Lambda).$$

Defining an operator makes a few statements about the cascade structure easy to formulate. First, a few basic lemmas will be introduced. Unless otherwise noted, it can be assumed that all functions are real-valued and twice-differentiable.

Definition: A function f is increasing on (a, b) if $f' \geq 0$ on (a, b). f is strictly increasing on (a, b) if $f' > 0$ on (a, b). f is (strictly) decreasing if $(-f)$ is (strictly) increasing.

Lemma 2.1.1 *1. Suppose that f and g are both increasing (decreasing). Then $f + g$ will be increasing (decreasing). If, in addition, f is strictly increasing (decreasing), then $f + g$ will be strictly increasing (decreasing).*

2. Suppose f is non-zero and (strictly) increasing (decreasing). Then $1/f$ will be (strictly) decreasing (increasing).

3. *Suppose that f and g are both positive and increasing (decreasing). Then fg will be increasing (decreasing). If f and g are both negative and increasing (decreasing), then fg will be decreasing (increasing). If f is negative and decreasing and g is positive and increasing, then fg will be decreasing.*

Proof: The proofs are straightforward by seeing that $(f+g)' = f' + g'$, and $\left(\frac{1}{f}\right)' = \frac{-f'}{f^2}$, and $(fg)' = f'g + g'f$. ∎

Definition: A function is concave on (a, b) if $f'' \leq 0$ on (a, b). A function is strictly concave if $f'' < 0$. A function f is (strictly) convex if $(-f)$ is (strictly) concave.

The concept of log-concavity will also be useful to introduce. Most of these statements can be found in [30].

Definition: A positive function f is log-concave on (a, b) if $\log(f)$ is concave on (a, b). A positive function f is strictly log-concave on (a, b) if $\log(f)$ is strictly concave on (a, b).

Remark: The strict log-concavity of f on (a, b) is equivalent to:

1. f'/f is strictly decreasing on (a, b).
2. $\log(f)'' < 0$ on (a, b).
3. f can be expressed as e^{ϕ} where ϕ is strictly concave on (a, b).

Lemma 2.1.2 *Suppose f is a strictly log-concave function on (a, b). Then f is unimodal on (a, b).*

Proof: It is easier to prove the contrapositive. Suppose f is not unimodal. Then $\exists m_1, m_2 \in (a, b)$ such that $m_1 < m_2$ and $f(m_1)$ and $f(m_2)$ are local maxima. Since

$f'(x)$ is continuous, $\exists m_3 \in (m_1, m_2)$ such that $f(m_3)$ is a local minimum. Since f is positive $\frac{f'(m_3)}{f(m_3)} = 0$. Also, since $f(m_3)$ is a local minimum, $\exists \epsilon > 0$ such that $f'(x) > 0$ for all $x \in (m_3, m_3 + \epsilon)$. This implies $\frac{f'(x)}{f(x)} > 0$ on $(m_3, m_3 + \epsilon)$. Then it must be that $\frac{f'}{f}$ increases at some point in the interval $[m_3, m_3 + \epsilon] \subset (a, b)$. Therefore, f is not strictly log-concave. ∎

Lemma 2.1.3 *Let g be a strictly monotonic function on (a, b). Suppose that $g(a) = 0$ or $g(b) = 0$. If g' is a strictly log-concave on (a, b), then g is also strictly log-concave on (a, b).*

The proof can be found in [30]. The basic idea is to use the Cauchy Mean-Value Theorem. Now some properties of F can be described.

Lemma 2.1.4 *Suppose that $\Lambda \in \Lambda_{set}$. Then the following is true.*

1. *For all $n \geq 1$, $F^n(\Lambda)$ will be an increasing function of T. Also, $F(\Lambda)$ can be extended to define a cumulative distribution function with semi-infinite support and $1 - F^n(\Lambda)$ can be extended to define the corresponding survival function.*

2. *For all $n \geq 2$, $F^n(\Lambda)$ will be a strictly increasing function of T. $1 - F^n(\Lambda)$ will be log-concave on $(0, \infty)$.*

3. *For all $n \geq 3$, $1 - F^n(\Lambda)$ will be strictly log-concave on $(0, \infty)$.*

4. *If Λ is strictly increasing and log-concave, then for all $n \geq 1$, $F^n(\Lambda)$ will have a strictly log-concave derivative. This also means that the derivative of $F^n(\Lambda)$ will be unimodal and $F^n(\Lambda)$ will be strictly log-concave.*

Proof: To prove 1, consider $f(T) = 1 - \exp(-T)$. It is easy to show that f is strictly increasing and that $f(0) = 0$ and $\lim_{t\to\infty} f(T) = 1$. If $\Lambda \in \Lambda_{set}$, then $f\left(\int_0^T \Lambda(x)dx\right)$ will be increasing. It can be shown by induction that $F^n(\Lambda)$ will be increasing. Let

$p(T) = (F(\Lambda))(T)$ for $T \geq 0$. Let $p(T) = 0$ for all $T < 0$. Then p will be an increasing function such that $p(\infty) = 1$ and $p(0) = 0$. Also, since Λ is non-zero in a half-interval about 0, it can be seen by the definition of F that p will be positive on $(0, \infty)$. Therefore, p will be a cumulative distribution function with support on $(0, \infty)$. By induction, $p^n(T)$ will also be a cumulative distribution function with support on $(0, \infty)$.

To prove 2, let $p_1 = F(\Lambda)$, $p_2 = F(p_1)$, and $s_2 = 1 - p_2$. From 1, p_1 is increasing and positive on $(0, \infty)$. Therefore, $\int_0^T p_1(x)dx$ is strictly increasing. Therefore, $F(p_1) = p_2$ will be strictly increasing. s_2 can be expressed as e^{ϕ} where $\phi(T) = -\int_0^T p_1(x)dx$. Then $\phi' = -p_1$ and $\phi'' = -p_1'$. Since p_1 is increasing, $\phi'' \leq 0$. Therefore, s_2 will be log-concave on $(0, \infty)$. By induction, $F^n(\Lambda)$ will be strictly increasing and $1 - F^n(\Lambda)$ will be log-concave for all $n \geq 2$.

To prove 3, let $p_3 = F^3(\Lambda)$ and $s_3 = 1 - p_3$. By the same argument above, $s_3 = e^{\phi}$ where $\phi'' = -p_2'$. Since p_2 is strictly increasing, $\phi'' < 0$.

Finally, to prove 4, suppose that Λ is log-concave and strictly increasing. Let $p = F(\Lambda)$, $s = 1 - p$, and $c = p' = -s'$. From the same argument above, it can be shown that s is strictly log-concave. It can be shown that:

$$\frac{c'}{c} = \frac{\Lambda'}{\Lambda} + \frac{s'}{s}.$$

Since Λ is log-concave and s is strictly log-concave, $\frac{\Lambda'}{\Lambda}$ and $\frac{s'}{s}$ are a decreasing function and a strictly decreasing function respectively. By Lemma 2.1.1, $\frac{c'}{c}$ will be strictly decreasing. Therefore, c is strictly log-concave. By Lemma 2.1.2, c is unimodal. By Lemma 2.1.3, p will be strictly log-concave and will also by strictly increasing as argued above. By induction, this will be true for all $n \geq 1$. ∎

The following conjecture is motivated by simulations:

Conjecture: Suppose that $\Lambda \in \Lambda_{set}$. Then there $\exists k \in \mathbb{N}$ such that $F^n(\Lambda)$ will have a strictly log-concave and unimodal derivative for all $n \geq k$.

Based on Lemma 2.1.4, it would suffice to show that $F^k(\Lambda)$ becomes log-concave for some k. What is interesting is that this conjecture can be naturally extended to define a conjecture in probability theory. Similar conjectures in probability theory have been stated that deal with the n-fold convolution of unimodal densities [31].

2.1.1 Simulation Results and Discussion

Figure 2.2 shows that even a simple enzymatic cascade can convert a wide variety of input signals into a smooth, sigmoidal progression curve, and this is typically done within 3 iterations. This leads to the conjecture that there exists a finite stage cascade that can convert every signal from Λ_{set} into a sigmoidal output. The simulations also show that multiple stages can decrease the activation time, the time it takes for the product concentration to approach a quasi-steady state. However, this is only true up to a point, after which increasing the number of layers will only delay the activation time. This result is dependent on the modules being identical.

Many properties of the function operator have yet to be proven, such as: Given an input, how many iterations would be needed for an optimal activation time, i.e. after how many stages will the activation start moving to the right, and is the "shift" to the right eventually constant? It appears that these questions can be answered by examining iterating functions of the type:

$$1 - \exp\left(-\int_0^t \Lambda(x)dx\right).$$

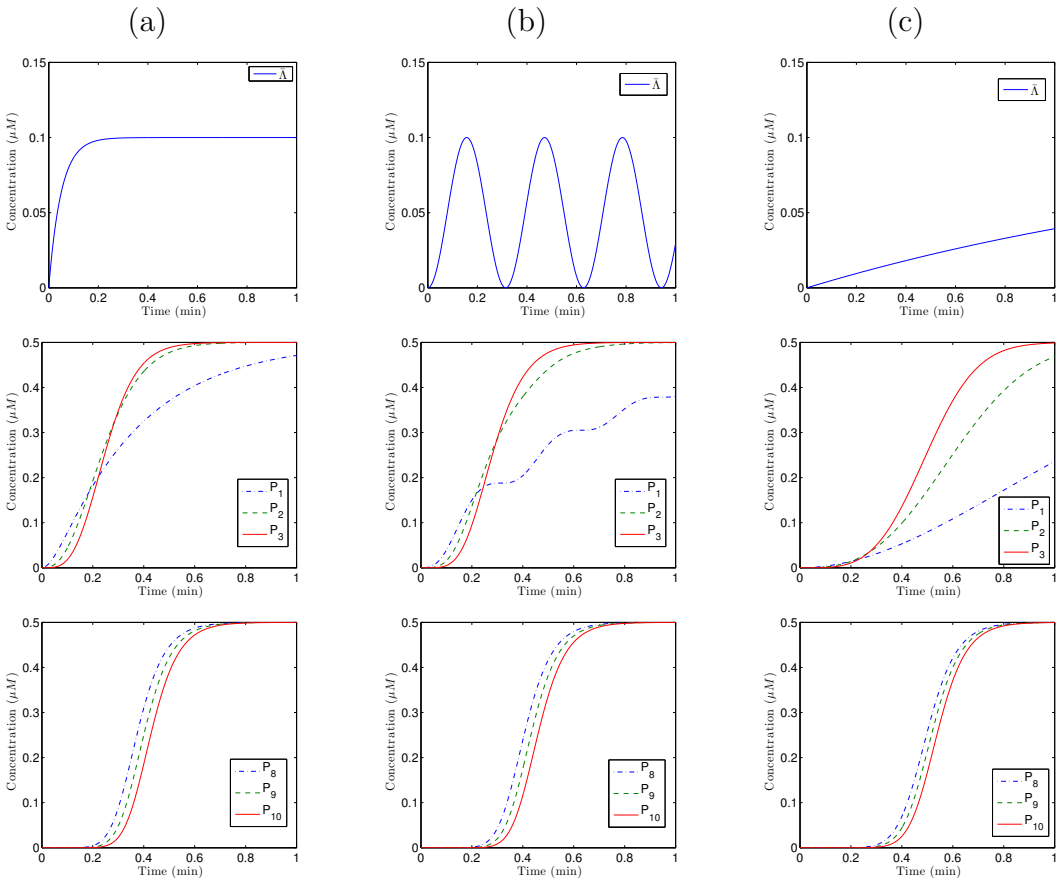

Figure 2.2: Plots of various inputs and their outputs for a basic enzymatic cascade with identical modules. In the first row, various input signals are plotted. In column (a), $\bar{\Lambda} = \bar{E}\,(1 - \exp(-\omega t))$ with $\omega = 20\ min^{-1}$. In column (b), $\bar{\Lambda} = \bar{E}\,(1 - \cos(\omega t))\,/2$ with $\omega = 20\ min^{-1}$. In column (c), $\bar{\Lambda} = \bar{E}\,(1 - \exp(-\omega t))$ with $\omega = 0.5\ min^{-1}$. Equation (2.1) was integrated for the various inputs with $\bar{E} = 0.1\mu M$, $\bar{S}_i = 0.5\mu M$, and $a_i = 30(\mu M\, min)^{-1}$. The second row shows that various inputs have a sigmoidal output after three layers and that the activation time moves to the left. The last row shows what an 8, 9, and 10 layer cascade would do to the input. Eventually, the activation time moves to the right.

2.2 Enzymatic Cascade with Complex Formation

The enzymatic cascade seen in Figure 2.1 can be made more relevant by adding intermediate complex formation. An n-stage cascade would have the following stoichiometry:

$$
\begin{aligned}
\varnothing &\xrightarrow{\bar{\lambda}(t)} E, \\
E + S_1 &\underset{d_1}{\overset{a_1}{\rightleftarrows}} C_1 \xrightarrow{k_1} E + P_1, \\
P_1 + S_2 &\underset{d_2}{\overset{a_2}{\rightleftarrows}} C_2 \xrightarrow{k_2} P_1 + P_2, \\
&\vdots \\
P_{n-1} + S_n &\underset{d_n}{\overset{a_n}{\rightleftarrows}} C_n \xrightarrow{k_n} P_{n-1} + P_n.
\end{aligned}
$$

The corresponding set of mass-action equations is:

$$
\begin{aligned}
\dot{E} &= \bar{\lambda}(t) - a_1 E S_1 + (d_1 + k_1) C_1, \\
\dot{S}_1 &= -a_1 E S_1 + d_1 C_1, \\
\dot{C}_1 &= a_1 E S_1 - (d_1 + k_1) C_1, \\
\dot{P}_1 &= k_1 C_1 - a_2 P_1 S_2 + (d_2 + k_2) C_2, \\
\dot{S}_2 &= -a_2 P_1 S_2 + d_2 C_2, \\
\dot{C}_2 &= a_2 P_1 S_2 - (d_2 + k_2) C_2, \\
\dot{P}_2 &= k_2 C_2 - a_3 P_2 S_3 + (d_3 + k_3) C_3, \\
&\vdots \\
\dot{S}_n &= -a_n P_{n-1} S_n + d_n C_n, \\
\dot{C}_n &= a_n P_{n-1} S_n - (d_n + k_n) C_n, \\
\dot{P}_n &= k_n C_n, \\
E(0) = C_i(0) = P_i(0) &= 0, \quad S(0) = \bar{S}_i, \quad \text{for } 1 \leq i \leq n.
\end{aligned}
\tag{2.8}
$$

As before, system (2.8) will be expressed as a sequence of modules given by the stoichiometry:

$$
\begin{aligned}
\varnothing &\xrightarrow{\bar{\lambda}(t)} E \\
E + S &\underset{d_1}{\overset{a_1}{\rightleftarrows}} C \xrightarrow{k_1} E + P.
\end{aligned}
$$

The corresponding set of mass-action equations is:

$$\begin{aligned}
\dot{E} &= \bar{\lambda}(t) - a_1 ES + (d_1 + k_1)C, \\
\dot{S} &= -a_1 ES + d_1 C, \\
\dot{C} &= a_1 ES - (d_1 + k_1)C, \\
\dot{P} &= k_1 C, \\
E(0) = C(0) = P(0) &= 0, \quad S(0) = \bar{S}.
\end{aligned} \tag{2.9}$$

Mass-conservation can be used to reduce system (2.9).

$$\begin{aligned}
S_C &= S + C, \\
E + C &= \int_0^t \bar{\lambda}(x)dx =: \bar{\Lambda}(t), \\
P &= \bar{S} - S_C, \\
\dot{S}_C &= -k_1 C, \\
\dot{C} &= a_1(\bar{\Lambda} - C)(S_C - C) - (d_1 + k_1)C, \\
C(0) = 0, &\quad S_C(0) = \bar{S}.
\end{aligned} \tag{2.10}$$

The system will be scaled to analyze the total substrate concentration S_C and the product formation P, which will provide a way to apply perturbation techniques. $\bar{\Lambda}$, which represents the total enzyme concentration in the system, can be assumed to be non-negative and bounded. As before, say

$$\sup_{t\in[0,\infty)} \{\bar{\Lambda}(t)\} = \bar{E} < \infty.$$

To get an estimate for the maximum of C to provide a scaling parameter, it will be necessary to first show that such a maximum exists. It can be argued physically, or

by examining:

$$\begin{aligned} \dot{S} &= -a_1(\bar{\Lambda} - C)S + d_1 C, \\ \dot{C} &= a_1(\bar{\Lambda} - C)S - (d_1 + k_1)C, \\ C(0) &= 0, \quad S(0) = \bar{S}, \end{aligned} \tag{2.11}$$

that C and S will stay non-negative. If $C = S = 0$, then $\dot{S} = \dot{C} = 0$. If $S > 0$ and $C = 0$, then $\dot{C} \geq 0$ since $\bar{\Lambda} \geq 0$. If $S = 0$ and $C > 0$, then $\dot{S} > 0$. The right hand side of system (2.11) is continuous with continuous partials, so the solution set will be unique and continuous. So solutions that start in the first quadrant will stay in the first quadrant. Since C is bounded, it must have a supremum. Also, if $\dot{C}(t_0) > 0$, then it must be that there exists $t_1 > t_0$ such that $\dot{C}(t_1) < 0$. If not, then there would exist an $\epsilon > 0$ and $t_2 > t_0$ such that $C(t) > \epsilon$ for all $t > t_2$. Then that would suggest $S_C < K - k_1\epsilon(t - t_2)$ for some $K > 0$ and for all $t > t_2$. t could be made large enough such that $S_C < 0$, which cannot happen. Therefore, there is a local maximum of C that is arbitrarily close to the supremum. Let t_{max} be the point of such a local maximum. Then

$$\dot{C}(t_{max}) = 0 = a_1(\bar{\Lambda}(t_{max}) - C(t_{max}))S(t_{max}) - (d_1 + k_1)C(t_{max}).$$

This implies

$$C(t_{max}) = \frac{\bar{\Lambda}(t_{max})S(t_{max})}{K_m + S(t_{max})} \leq \frac{\bar{E}\bar{S}}{K_m + \bar{S}} =: \bar{C}, \tag{2.12}$$

where

$$K_m = \frac{d_1 + k_1}{a_1} \tag{2.13}$$

is the Michaelis-Menten parameter.

The timescale on which the total-substrate concentration operates on can be estimated by:

$$\frac{(S_{C_{max}} - S_{C_{min}})}{\left|\dot{S}_C\right|_{max}} \approx \frac{\bar{S}}{k_1\bar{C}} = \frac{K_m + \bar{S}}{k_1\bar{E}} := t_{S_C}. \tag{2.14}$$

The variables in system (2.10) can be scaled as:

$$T = \frac{t}{t_{S_C}}, \quad s_c(T) = \frac{S_C(t)}{\bar{S}}, \quad c(T) = \frac{C(t)}{\bar{C}}, \quad p(T) = \frac{P(t)}{\bar{S}}, \quad \Lambda(T) = \frac{\bar{\Lambda}(t)}{\bar{E}}.$$

The following dimensionless parameters will be needed:

$$\sigma = \frac{\bar{S}}{K_m}, \quad \kappa = \frac{d_1}{k_1}, \quad \epsilon = \frac{\bar{E}}{K_m + \bar{S}}.$$

System (2.10) is equivalent to the following dimensionless system:

$$\begin{aligned}
\Lambda(T) &= \frac{1}{\bar{E}} \int_0^{t_s T} \bar{\lambda}(x) dx, \\
p(T) &= 1 - s(T), \\
s_c'(T) &= -c, \\
\epsilon c'(T) &= (\kappa + 1) \left[((\sigma + 1)\Lambda(T) - \sigma c)(s_c - \epsilon c) - c \right], \\
s_c(0) &= 1, \quad c(0) = 0.
\end{aligned} \tag{2.15}$$

If it is assumed that $\epsilon << 1$, then perturbation theory can be applied to approximate system (2.15). Suppose that s_c and c can be expanded in powers of ϵ,

$$\begin{aligned}
s_c(T) &\sim s_{c_0}(T) + \epsilon s_{c_1}(T) + \cdots, \\
c(T) &\sim c_0(T) + \epsilon c_1(T) + \cdots.
\end{aligned}$$

Then the $O(1)$ equations are:

$$\begin{aligned}
s_{c_0}' &= -c_0, \\
c_0 &= \frac{(\sigma + 1)\Lambda(T) s_{c_0}}{\sigma s_{c_0} + 1}, \\
s_{c_0}(0) &= 1, \quad c_0(0) = 0.
\end{aligned} \tag{2.16}$$

The system (2.16) has an explicit solution:

$$\begin{aligned}
s_{c_0}(T) &= \frac{1}{\sigma} W \left[\sigma \exp\left(\sigma - (1 + \sigma) \int_0^T \Lambda(x) dx \right) \right], \\
p_0(T) &= 1 - \frac{1}{\sigma} W \left[\sigma \exp\left(\sigma - (1 + \sigma) \int_0^T \Lambda(x) dx \right) \right],
\end{aligned} \tag{2.17}$$

where W is the Lambert-W function. By examining the properties of the Lambert-W function and the exponential function, it can be shown that the functional operator:

$$F : (\Lambda_{set}, \mathbb{R}_{>0}) \to \Lambda_{set},$$

defined as:

$$F_\sigma(\Lambda) = 1 - \frac{1}{\sigma} W\left[\sigma \exp\left(\sigma - (1+\sigma)\int_0^T \Lambda(x)dx\right)\right] \tag{2.18}$$

is well-defined. Let

$$F^1(\Lambda) = F_{\sigma_1}(\Lambda), \quad F^2(\Lambda) = F_{\sigma_2}(F_{\sigma_1}(\Lambda)), \quad \cdots .$$

Then the output for an n-stage cascade is approximated by:

$$p_{0n} = F^n(\Lambda).$$

Lemma 2.2.1 *The same conclusions in Lemma 2.1.4 will also be true for the operator defined in* (2.18).

Proof: The proofs to show that every iterate will be increasing and every iterate after the first will be strictly increasing are very similar to the proofs for Lemma 2.1.4 but now considering $f(T,\sigma) = 1 - \frac{1}{\sigma} W\left[\sigma \exp\left(\sigma - (1+\sigma)T\right)\right]$. It is easy to show that $f(0,\sigma) = 0$, $\lim_{T\to\infty} f(T,\sigma) = 1$, and $f(T,\sigma)$ is strictly increasing in T.

To prove the log-concavity assertions, let $p_1 = F^1(\Lambda)$, $p_2 = F^2(\Lambda)$, and $s_{c_2} = 1 - p_2$. From the system (2.16),

$$\frac{s'_{c_2}}{s_{c_2}} = \frac{-(\sigma_2+1)p_1}{\sigma_2 s_{c_2} + 1}.$$

Since s_{c_2} is decreasing and positive, $\frac{\sigma_2+1}{\sigma_2 s_{c_2}+1}$ will be increasing and positive. Since p_1 is increasing and positive, by Lemma 2.1.1 $\frac{s'_{c_2}}{s_{c_2}}$ will be decreasing. A similar argument can be made to show that s_{c_3} will be strictly log-concave.

To prove assertion 4, let $p = F^1(\Lambda)$, $c = p'$, and $s_c = 1 - p$. It can be shown that:

$$\frac{c'}{c} = \frac{\Lambda'}{\Lambda} + \frac{s'_c}{(\sigma_1 s_c + 1)s_c}.$$

It was argued above that s_c will be log-concave, so $\frac{s_c'}{s_c}$ will be decreasing and negative since $s_c' < 0$ and $s_c > 0$. This also implies that $\frac{1}{\sigma_1 s_c + 1}$ will be increasing and positive. By Lemma 2.1.1, $\frac{c'}{c}$ will be log-concave and unimodal. This implies p will be log-concave by Lemma 2.1.2. Induction can then be applied. ∎

This motivates a more general probability conjecture.

Conjecture: Suppose ϕ is a differentiable, log-concave cumulative distribution function with support on $(0, \infty)$. Let Λ be a cumulative distribution function with support on $(0, \infty)$. Let $F(\Lambda) = \phi\left(\int_0^x \Lambda(t)dt\right)$. Then there exists $k \in \mathbb{N}$ such that $F^n(\Lambda)$ has a unimodal density for all $n \geq k$.

2.2.1 Accuracy of the perturbation scheme

To determine the accuracy of system (2.16) to approximate system (2.15), the $O(\epsilon)$ equations can be analyzed. It will be useful to note that

$$c_0' = \frac{(\sigma+1)s_{c_0}\Lambda'}{\sigma s_{c_0}+1} + \frac{(\sigma+1)s_{c_0}'\Lambda}{(\sigma s_{c_0}+1)^2}. \tag{2.19}$$

The $O(\epsilon)$ equations are:

$$\begin{aligned} c_1 &= \frac{1}{1+\sigma s_{c_0}}\left(c_0(\sigma c_0 - (\sigma+1)\Lambda) + ((\sigma+1)\Lambda - \sigma c_0)s_{c_1} - \frac{c_0'}{\kappa+1}\right), \\ s_{c_1}' &= -c_1, \\ s_{c_1}(0) &= 0. \end{aligned}$$

The equation for s_{c_1} can be expressed as:

$$s_{c_1}' = -P(T)s_{c_1} + Q(T),$$

where

$$P(T) = \frac{1}{1+\sigma s_{c_0}}((\sigma+1)\Lambda - \sigma c_0) = \frac{-s'_{c_0}}{s_{c_0}} + \frac{\sigma s'_{c_0}}{1+\sigma s_{c_0}},$$
$$Q(T) = \frac{1}{1+\sigma s_{c_0}}\left(\frac{c'_0}{\kappa+1} + c_0((\sigma+1)\Lambda - \sigma c_0)\right)$$
$$= \frac{1}{1+\sigma s_{c_0}}\left(\frac{(\sigma+1)s_{c_0}\Lambda'}{(\kappa+1)(\sigma s_{c_0}+1)} + \frac{(\sigma+1)s'_{c_0}\Lambda}{(\kappa+1)(\sigma s_{c_0}+1)^2} - (\sigma+1)\Lambda s'_{c_0} + \frac{\sigma s'_{c_0}(\sigma+1)s_{c_0}\Lambda}{\sigma s_{c_0}+1}\right).$$

This means

$$s_{c_1} = \exp\left(-\int_0^T P(x)dx\right)\int_0^T \exp\left(\int_0^y P(x)dx\right)Q(y)dy.$$

The integrating factor is:

$$\exp\left(\int_0^T P(x)dx\right) = \frac{1+\sigma s_{c_0}}{(\sigma+1)s_{c_0}}.$$

Hence,

$$\exp\left(\int_0^T P(x)dx\right)Q(T) = \frac{\Lambda'}{(\kappa+1)(\sigma s_{c_0}+1)} + \Lambda\left(\frac{s'_{c_0}}{(\kappa+1)s_{c_0}(\sigma s_{c_0}+1)^2} - \frac{s'_{c_0}}{s_{c_0}(\sigma s_{c_0}+1)}\right).$$

Then

$$\int_0^T \exp\left(\int_0^y P(x)dx\right)Q(y)dy = \int_0^T \frac{\Lambda'}{(\kappa+1)(\sigma s_{c_0}+1)} + \Lambda\left(\frac{s'_{c_0}}{(\kappa+1)s_{c_0}(\sigma s_{c_0}+1)^2} - \frac{s'_{c_0}}{s_{c_0}(\sigma s_{c_0}+1)}\right)dy.$$

Let $u = s_{c_0}(y)$ and $v = \Lambda(y)$. Then

$$\int_0^T \exp\left(\int_0^y P(x)dx\right)Q(y)dy = \int_0^\Lambda \frac{1}{(\kappa+1)(\sigma u+1)}dv + \int_1^{s_{c_0}} \frac{v}{(\kappa+1)u(\sigma u+1)^2}du - \int_1^{s_{c_0}} \frac{v}{u(\sigma u+1)}du.$$

Since $0 \leq u, v \leq 1$,

$$\begin{aligned}
&\left| \int_0^T \exp\left(\int_0^y P(x)dx \right) Q(y)dy \right| \\
&\qquad \leq \frac{1}{\kappa+1} \int_0^\Lambda dv + \frac{1}{\kappa+1} \left| \int_1^{s_{c_0}} \frac{1}{u(\sigma u+1)^2} du \right| + \left| \int_1^{s_{c_0}} \frac{1}{u(\sigma u+1)} du \right| \\
&\qquad = \frac{\Lambda}{\kappa+1} + \frac{1}{\kappa+1} \left| \log\left(\frac{(\sigma+1)s_{c_0}}{\sigma s_{c_0}+1} \right) + \frac{\sigma(1-s_{c_0})}{(\sigma+1)(\sigma s_{c_0}+1)} \right| \\
&\qquad\qquad + \left| \log\left(\frac{(\sigma+1)s_{c_0}}{\sigma s_{c_0}+1} \right) \right|.
\end{aligned}$$

This implies the inequality:

$$\begin{aligned}
|s_{c_1}| &\leq \frac{(\sigma+1)s_{c_0}\Lambda}{(\sigma s_{c_0}+1)(\kappa+1)} + \frac{\sigma s_{c_0}(1-s_{c_0})}{(\kappa+1)(\sigma s_{c_0}+1)^2} \\
&\quad - \frac{(\sigma+1)s_{c_0}}{(\kappa+1)(\sigma s_{c_0}+1)} \log\left(\frac{(\sigma+1)s_{c_0}}{\sigma s_{c_0}+1} \right) - \frac{(\sigma+1)s_{c_0}}{\sigma s_{c_0}+1} \log\left(\frac{(\sigma+1)s_{c_0}}{\sigma s_{c_0}+1} \right) \\
&\leq \frac{1}{\kappa+1}\left(2 + \frac{1}{e}\right) + \frac{1}{e} < 3,
\end{aligned}$$

which implies that if $\epsilon << 1$, then $\epsilon\,|s_{c_1}| << 1$. Therefore, the perturbation scheme is valid.

Since F is an $O(1)$ approximation to the true output, treating a cascade as an n-fold iteration of F has the potential to introduce additional error. It is intuitive that one can trade the number of iterations against the smallness of ϵ.

We can see how perturbations in the input would propagate through the approximated model. Suppose Λ is the input and $\Lambda + \epsilon\Lambda_1$ is the perturbed input. Let s_{c_0} be the output for Λ and $\tilde{s}_{c_0}$ be the output to the perturbed input. Then

$$\begin{aligned}
\log(s_{c_0}) + \sigma s_{c_0} &= \sigma - (\sigma+1)\int_0^T \Lambda(x)dx, \\
\log(\tilde{s}_{c_0}) + \sigma \tilde{s}_{c_0} &= \sigma - (\sigma+1)\int_0^T \Lambda(x) + \epsilon\Lambda_1(x)dx,
\end{aligned}$$

which implies

$$\log(s_{c_0}) - \log(\tilde{s}_{c_0}) + \sigma(s_{c_0} - \tilde{s}_{c_0}) = (\sigma+1)\epsilon \int_0^T \Lambda_1(x)dx.$$

By the Mean Value Theorem, there exists $\xi \in (\tilde{s}_{c_0}, s_{c_0}) \subset (0, 1]$, such that

$$\log(s_{c_0}) - \log(\tilde{s}_{c_0}) = \frac{1}{\xi}(s_{c_0} - \tilde{s}_{c_0}).$$

This implies that

$$|s_{c_0} - \tilde{s}_{c_0}| = \left|\frac{\sigma + 1}{\sigma + 1/\xi}\right| \left|\epsilon \int_0^T \Lambda_1(x)dx\right| \leq \epsilon \left|\int_0^T \Lambda_1(x)dx\right|.$$

This suggests that using a sequence of function compositions as a model of a signaling cascade works well if $\left|\int_0^\infty s_1(x)dx\right|$ is bounded. Unfortunately, given the general properties of the input Λ, it can be shown that $\left|\int_0^\infty s_1(x)dx\right|$ can be made relatively large. It is possible to contrive counter-examples demonstrating a large error between the outputs with inputs that are $O(\epsilon)$ between each other, but for most relevant situations, the outputs tend to stay close to each other. More work is needed to determine exactly what additional properties of Λ would guarantee close outputs.

2.2.2 Simulation Results and Discussion

As can be seen in Figure 2.4, it appears that an enzymatic cascade with complex formation will process signals similarly to an enzymatic cascade without complex formation. Perturbation techniques were used to prove this fact when $\bar{E}/(\bar{S} + K_m)$ is small. In the process, a Michaelis-Menten type equation for open enzymatic systems was developed and rigorously analyzed. Figure 2.5 demonstrates the validity of the perturbation scheme even with a periodic input. Parameters derived from closed-enzymatic experiments should be applicable to open enzyme networks under certain conditions. It was shown that the error in the approximation to s_c, and hence p, will be small if ϵ is small. However, it is possible that the approximation to c could be large depending on Λ' and σ. If Λ' is large, then the error in c could be large. However, in the cascading scheme, the maximum possible slope of the output is always less

than one. It was shown that under certain conditions, errors in the input function will not propagate through a simple enzymatic reaction. Figure 2.6 shows that errors do tend to accumulate, but the rate appears linearly dependent on ϵ. More work is needed to analyze the error propagation into simple and complex enzymatic systems. It appears that iterating Equation (2.18) will convert any input into a sigmoidal output, and usually does so in 3 iterations. This result does not depend on having identical modules. A thousand simulations were run in which a 3-stage cascade had 3 different σ parameters randomly and uniformly sampled from 0 to 5. In all cases, the outputs were sigmoidal. Though a counterexample can be contrived to show a non-sigmoidal output for a 3-tier cascade, most physically relevant signals appear to be converted into a sigmoidal output. Figure 2.3 shows that the output curve for the counterexample is very close to being sigmoidal.

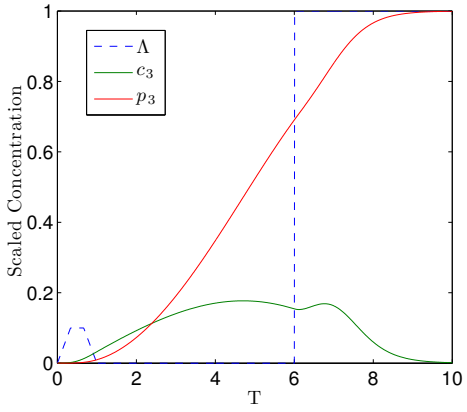

Figure 2.3: A non-sigmoidal counterexample for a 3 layer cascade. With a brief pulse input followed by a shock, a local maximum can be seen in the derivative of p_3. However, the output curve is essentially S-shaped. This result was generated by iterating Equation (2.18) with $\sigma = 1$.

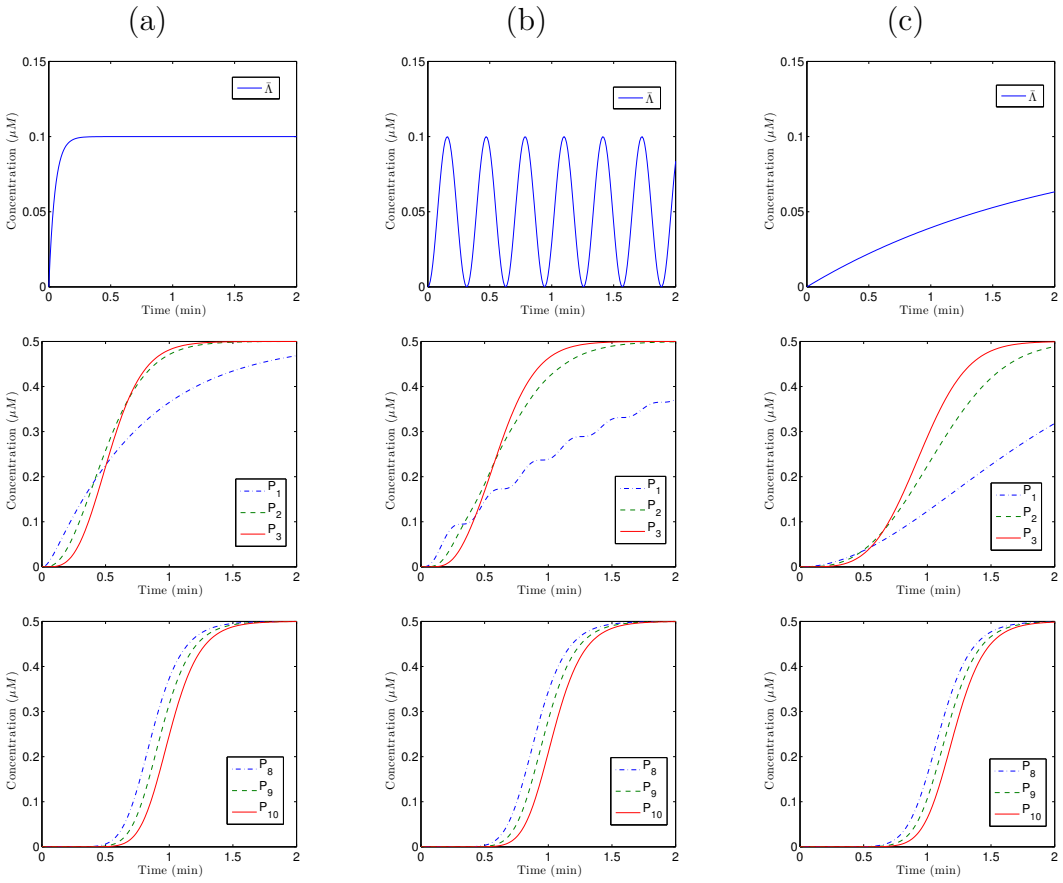

Figure 2.4: Plots of various inputs and their outputs for a basic enzymatic cascade with complex formation and identical modules. In the first row, various input signals are plotted. In column (a), $\bar{\Lambda} = \bar{E}\,(1 - \exp(-\omega t))$ with $\omega = 20\ min^{-1}$. In column (b), $\bar{\Lambda} = \bar{E}\,(1 - \cos(\omega t))\,/2$ with $\omega = 20\ min^{-1}$. In column (c), $\bar{\Lambda} = \bar{E}\,(1 - \exp(-\omega t))$ with $\omega = 0.5\ min^{-1}$. Equation (2.8) was integrated for the various inputs with $\bar{E} = 0.1\mu M$, $\bar{S}_i = 0.5\mu M$, $a_i = 30(\mu M\ min)^{-1}$, and $k_i = d_i = 60\ min^{-1}$ The second row shows that various inputs have a sigmoidal output after three layers and that the activation time moves to the left. The last row shows what an 8, 9, and 10 layer cascade would do to the input. Eventually, the activation time moves to the right. The results are very similar to the results for a more basic cascade without complex formation.

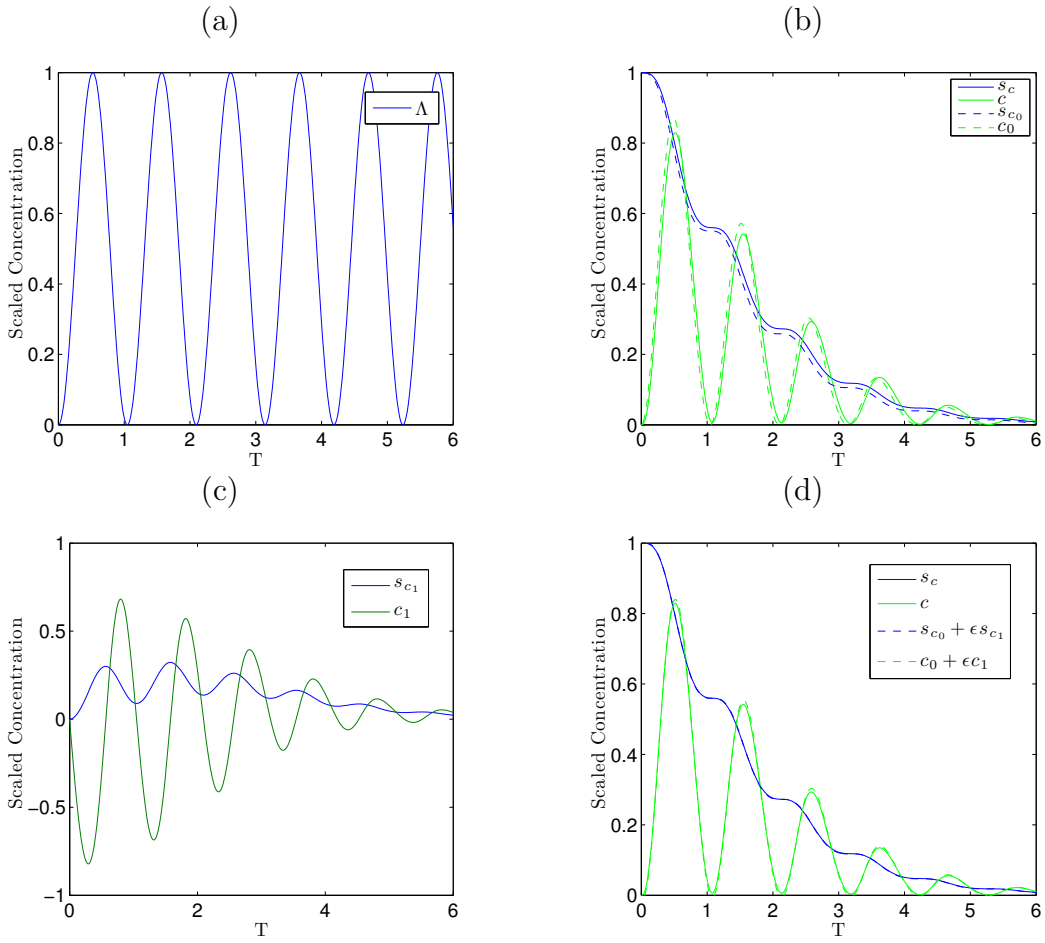

Figure 2.5: Plots demonstrating the accuracy of the perturbation expansion. In (a), the scaled input $\Lambda = (1 - \cos(\omega T))/2$ with $\omega = 6$ is plotted. Equation (2.15) and its $O(1)$ and $O(\epsilon)$ approximations were integrated with $\sigma = 1$, $\kappa = 1$, and $\epsilon = 0.1$.

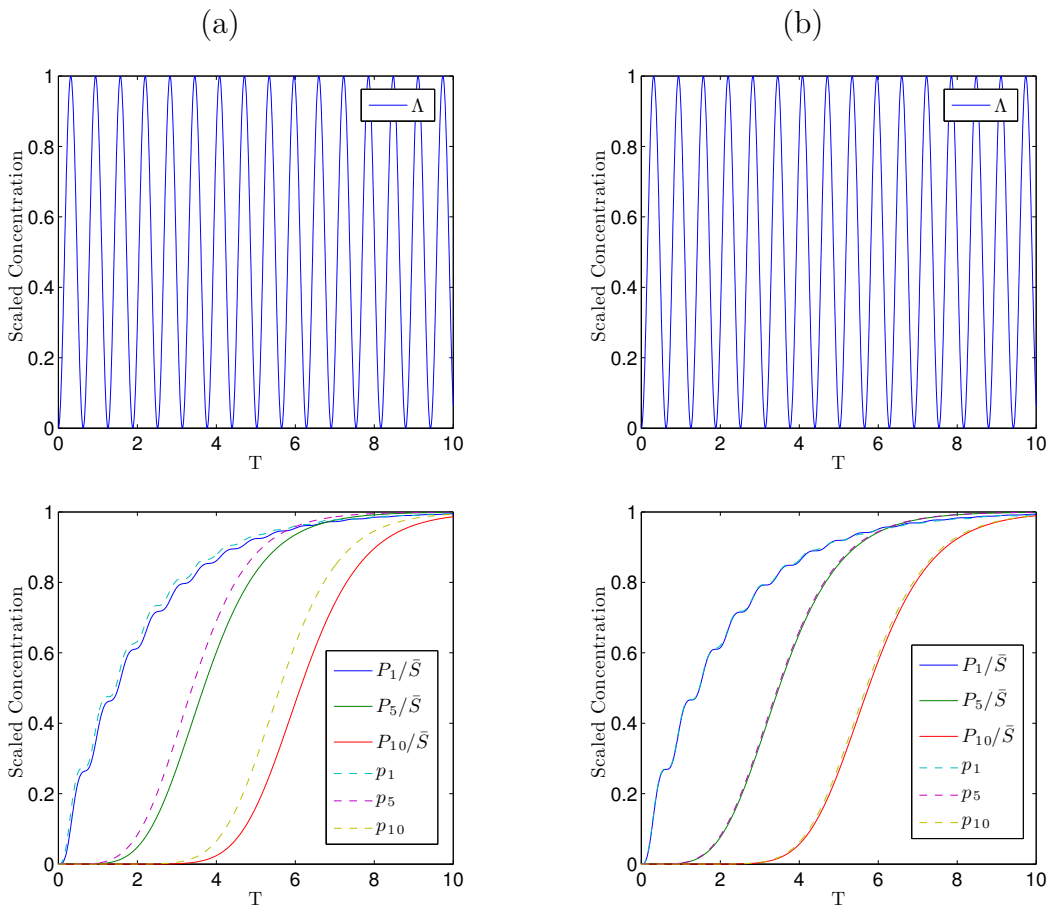

Figure 2.6: Plots demonstrating the accuracy of approximating an enzymatic cascade. The first row shows that the same input function is used; $\bar{\Lambda} = \bar{E}\left(1 - \cos(\omega t)\right)/2$ with $\omega = 10\ min^{-1}$. Equation (2.8) was integrated and scaled and then compared to iterating Equation (2.18). For simplicity, the rate parameters were derived from the parameters $\bar{E} = 0.5\mu M$, $\bar{S}_i = 0.5\mu M$, $\kappa = 1$, and $t_{s_c} = 1$. In column (a), $\epsilon = 0.1$. In column (b), $\epsilon = 0.01$. It appears that the errors tend to accumulate, but more work is needed to determine exactly at what rate the accumulation occurs.

2.3 Model of Enzymatic Cascade with Enzyme Destruction

The previous models assumed that the enzymes flowed into and out of the system at a rate independent of the enzyme concentration. It is possible to construct a cascade where the enzyme destruction is dependent on the enzyme concentration as seen in Figure 2.7. Suppose that the enzyme destruction is proportional to the

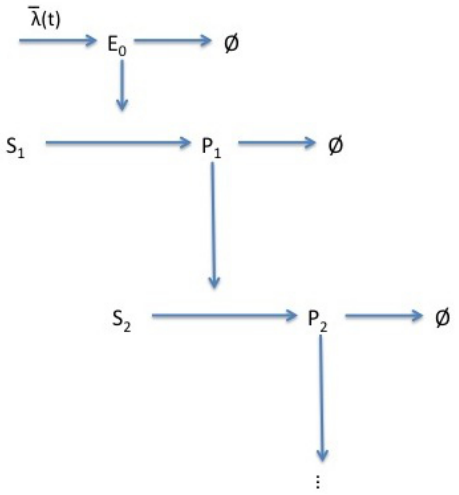

Figure 2.7: A basic enzymatic cascade where the enzymes are destroyed.

concentration of enzymes and that the final product, P_n, is not destroyed. Then the

stoichiometry is:

$$\begin{gathered}
\varnothing \underset{\tilde{d}_0}{\overset{\bar{\lambda}(t)}{\rightleftarrows}} E, \\
E + S_1 \xrightarrow{a_1} E + P_1, \\
P_1 \xrightarrow{\tilde{d}_1} \varnothing, \\
P_1 + S_2 \xrightarrow{a_2} P_1 + P_2, \\
P_2 \xrightarrow{\tilde{d}_2} \varnothing, \\
\vdots \\
P_{n-1} + S_n \xrightarrow{a_n} P_{n-1} + P_n.
\end{gathered}$$

The corresponding set of mass-action equations is:

$$\begin{aligned}
\dot{E} &= \bar{\lambda}(t) - \tilde{d}_0 E, \\
\dot{S}_1 &= -a_1 E S_1, \\
\dot{P}_1 &= a_1 E S_1 - \tilde{d}_1 P_1, \\
\dot{S}_2 &= -a_2 P_1 S_2, \\
\dot{P}_2 &= a_2 P_1 S_2 - \tilde{d}_2 P_2, \\
&\vdots \\
\dot{S}_n &= -a_n P_{n-1} S_n, \\
\dot{P}_n &= a_n P_{n-1} S_n, \\
E(0) = P_i(0) &= 0, \quad S(0) = \bar{S}_i, \quad \text{for } 1 \leq i \leq n.
\end{aligned} \tag{2.20}$$

If this cascade is represented as a chain of modules, each module would have the stoichiometry:

$$\begin{gathered}
\varnothing \underset{\tilde{d}_0}{\overset{\bar{\lambda}(t)}{\rightleftarrows}} E, \\
E + S \xrightarrow{a_1} E + P,
\end{gathered}$$

and the corresponding set of equations:

$$\begin{aligned}
\dot{E} &= \bar{\lambda}(t) - \tilde{d}_0 E, \\
\dot{S} &= -a_1 E S, \\
\dot{P} &= a_1 E S, \\
E(0) = P(0) = 0, &\quad S(0) = \bar{S}.
\end{aligned} \tag{2.21}$$

System (2.21) can be reduced to:

$$\begin{aligned}
P &= \bar{S} - S, \\
\dot{E} &= \bar{\lambda}(t) - \tilde{d}_0 E, \\
\dot{S} &= -a_1 E S, \\
E(0) = 0, &\quad S(0) = \bar{S}.
\end{aligned} \tag{2.22}$$

Let

$$\bar{\Lambda} = \int_0^t \bar{\lambda}(x) dx.$$

Suppose that $\bar{\Lambda}$ is non-negative and bounded and that

$$\sup_{t \in [0,\infty)} \{\bar{\Lambda}(t)\} = \bar{E} < \infty.$$

Unlike the previous models, there is no guarantee that all the substrates will be converted to products. So it will be difficult to derive a time-scale based on system (2.22) alone. Since $|S_{max} - S_{min}| \leq \bar{S}$, the following will be used to estimate the timescale:

$$\frac{|S_{max} - S_{min}|}{\left|\dot{S}\right|_{max}} \leq \frac{\bar{S}}{\left|\dot{S}\right|_{max}} \approx \frac{\bar{S}}{a_1 \bar{E} \bar{S}} = \frac{1}{a_1 \bar{E}} := t_s.$$

The variables in system (2.22) will be scaled as:

$$T = \frac{t}{t_s}, \quad s(T) = \frac{S(t)}{\bar{S}}, \quad p(T) = \frac{P(t)}{\bar{P}}, \quad m(T) = \frac{E(t)}{\bar{E}}, \quad \Lambda(T) = \frac{\bar{\Lambda}(t)}{\bar{E}},$$

with the following dimensionless parameter:

$$\eta = \frac{\tilde{d}_0}{a_1 \bar{E}}.$$

The scale for P, which is $\bar{P}$, will be determined later. The dimensionless system equivalent to system (2.22) is:

$$\begin{aligned} m' &= \Lambda'(T) - \eta m \\ s' &= -ms \\ m(0) = 0, &\quad s(0) = 1. \end{aligned} \tag{2.23}$$

System (2.23) can be solved explicitly.

$$\begin{aligned} m &= \Lambda(T) - \eta e^{-\eta T} \int_0^T e^{\eta x} \Lambda(x) dx \\ s &= \exp\left[- \int_0^T \Lambda(x) - \eta e^{-\eta x} \left(\int_0^x e^{\eta y} \Lambda(y) dy \right) dx \right]. \end{aligned}$$

Alternatively,

$$\begin{aligned} m &= e^{-\eta T} \int_0^T e^{\eta x} \Lambda'(x) dx \\ s &= \exp\left[- \int_0^T e^{-\eta x} \left(\int_0^x e^{\eta y} \Lambda'(y) dy \right) dx \right]. \end{aligned}$$

In the previous models, it was assumed that the enzymes flowed into and out of the system at a rate independent of the concentrations of the enzymes in the system. In this model, the destruction of the enzymes are proportional to the concentration of enzymes. So it will be assumed that flow into the system is positive. In addition, suppose that Λ satisfies most of the properties of (2.6). Let Λ_{set2} be the set of increasing functions that are in Λ_{set}. Then Λ will satisfy:

$$\lim_{T \to \infty} \Lambda(T) = 1.$$

The limiting behavior of s can be determined using a Laplace transform:

$$\begin{aligned}\lim_{T\to\infty} s(T) &= \exp\left[-\int_0^\infty e^{-\eta x}\left(\int_0^x e^{\eta y}\Lambda'(y)dy\right)dx\right] \\ &= \exp\left[-\mathcal{L}_x\left\{\int_0^x e^{\eta y}\Lambda'(y)dy\right\}(\eta)\ \right] \\ &= \exp\left(\frac{-\Lambda(\infty)}{\eta}\right) \\ &= \exp\left(\frac{-1}{\eta}\right).\end{aligned}$$

Therefore, the scale for the product can be determined as:

$$p(T) = \frac{P(t)}{\bar{S}\left(1-e^{-1/\eta}\right)},$$

and

$$p = \frac{1-s}{1-e^{-1/\eta}}.$$

One of the interesting differences between a model where the enzymes are destroyed and the previous models is that there is no guarantee all the substrates will be converted to products. In fact, it is possible that successive iterations of identical modules could have the opposite effect of amplification. Let

$$\gamma = \frac{a_1}{\tilde{d}_0}.$$

Then the supremum of $P(t)$ is:

$$\lim_{t\to\infty} P(t) = \bar{P} = \bar{S}\left(1-e^{-\gamma\bar{E}}\right). \tag{2.24}$$

Lemma 2.3.1 *Suppose a cascade is represented by system* (2.20) *with identical modules and module parameters* $\bar{S}$ *and* γ. *If* $\bar{S}\gamma \leq 1$, *then* $\lim_{n\to\infty}\bar{P}_n = 0$. *If* $\bar{S}\gamma > 1$, *then there exists* $\bar{E}_{crit}$ *such that* $\bar{E}_{crit} = \bar{S}\left(1-\exp(-\gamma\bar{E}_{crit})\right)$ *and* $\lim_{n\to\infty}\bar{P}_n = \bar{E}_{crit}$.

Proof: The supremum of the products at each stage can be determined by iterating Equation (2.24), which will define a discrete dynamical system defined in reference

[32]:

$$\bar{P}_{n+1} = \bar{S}\left(1 - e^{-\gamma \bar{P}_n}\right).$$

Let

$$f(x) = \bar{S}\left(1 - e^{-\gamma x}\right).$$

Then the following is true:

$$\begin{aligned}
\lim_{x\to\infty} f(x) &= \bar{S}, \\
f(0) &= 0, \\
f'(x) &= \bar{S}\gamma e^{-\gamma x} > 0, \\
f'(0) &= \bar{S}\gamma, \\
f''(x) &= -\bar{S}\gamma^2 e^{-\gamma x} < 0.
\end{aligned}$$

Hence, f starts at 0, is increasing, bounded, and concave. If $f'(0) = \bar{S}\gamma \leq 1$, then 0 is the unique fixed point to the equation:

$$x = f(x),$$

and it will also be globally attracting. Therefore,

$$\lim_{n\to\infty} \bar{P}_{n+1} = 0.$$

Now suppose that that $f'(0) = \bar{S}\gamma > 1$. Then 0 will be an unstable fixed point for the iterative map. Since $f(0) = 0$ and $f'(0) > 1$, there is a neighborhood about 0 such that $f(x) > x$. Since f is bounded, increasing, and concave, there is a unique solution to $x = f(x)$, which shall be called $\bar{E}_{crit}$. So $\bar{E}_{crit} = \bar{S}\left(1 - \exp(-\gamma \bar{E}_{crit})\right)$. Also

$$f'(\bar{E}_{crit}) = \bar{S}\gamma e^{-\gamma \bar{E}}.$$

It is not difficult to argue using a Taylor Series expansion that:

$$\gamma \bar{E}_{crit} < e^{-\gamma \bar{E}_{crit}} - 1 \text{ for } \gamma \bar{E}_{crit} > 0.$$

This implies that

$$\frac{\gamma \bar{E}_{crit} e^{-\gamma \bar{E}_{crit}}}{1 - e^{-\gamma \bar{E}}} < 1 \text{ and } f'(\bar{E}_{crit}) = \bar{S}\gamma e^{-\gamma \bar{E}} < 1.$$

So E_{crit} will be a globally attracting fixed point to the iterative map. Therefore, $\lim_{n\to\infty} \bar{P}_n = \bar{E}_{crit}$. ∎

Lemma 2.3.2 *Suppose a cascade is represented by system* (2.20) *and has alternating modules with parameters* $\bar{S}_1$, γ_1, $\bar{S}_2$, *and* γ_2. *If* $\bar{S}_1\bar{S}_2\gamma_1\gamma_2 \leq 1$, *then 0 will be a globally attracting fixed point. Otherwise, 0 will be an unstable fixed point.*

Proof: Let $f_1(x) = \bar{S}_1\left(1 - e^{-\gamma_1 x}\right)$ and $f_2(x) = \bar{S}_2\left(1 - e^{-\gamma_2 x}\right)$. Then

$$(f_1 \circ f_2)'(0) = (f_2 \circ f_1)'(0) = \bar{S}_1\bar{S}_2\gamma_1\gamma_2.$$

So $\lim_{n\to\infty} \bar{P}_n = 0$ if $\bar{S}_1\bar{S}_2\gamma_1\gamma_2 \leq 1$, and 0 will be unstable otherwise. ∎

2.3.1 Simulation Results and Discussion

Depending on the enzyme destruction rate, a cascade with enzyme destruction can behave differently than a cascade without. There is no guarantee that all the substrates will converted into products. Column (a) of Figure 2.8 shows that if the enzyme destruction rate is small, then the steady-states of the outputs will approach an $\bar{E}_{crit}$ value with each additional layer. The shapes of the curves are sigmoidal and tend to shift to the right with each additional layer as seen in a basic enzymatic cascade. Column (b) of Figure 2.8 shows that if the enzyme destruction rate is high, then each additional layer in the cascade will actually cause the steady-states to decrease until they approach zero. To prove this and determine the relevant parameters, an iterative map was formulated. Figure 8 displays cobweb plots of different iterative schemes. Figure 8 (a) shows that if $\bar{S}\gamma < 1$, then the steady states will approach

a non-zero fixed point, which suggests the outputs can be amplified. Figure 8 (b) shows that if $\bar{S} > 1$, then zero will be a global attractor of the iterative map. Figure 8 (c) shows that if two different modules are alternated with $\bar{S}_1\bar{S}_2\gamma_1\gamma_2 > 1$, then the steady-states will eventually switch between two different non-zero values. Figure 8 (d) shows that if $\bar{S}_1\bar{S}_2\gamma_1\gamma_2 < 1$, then zero will again be a global attractor.

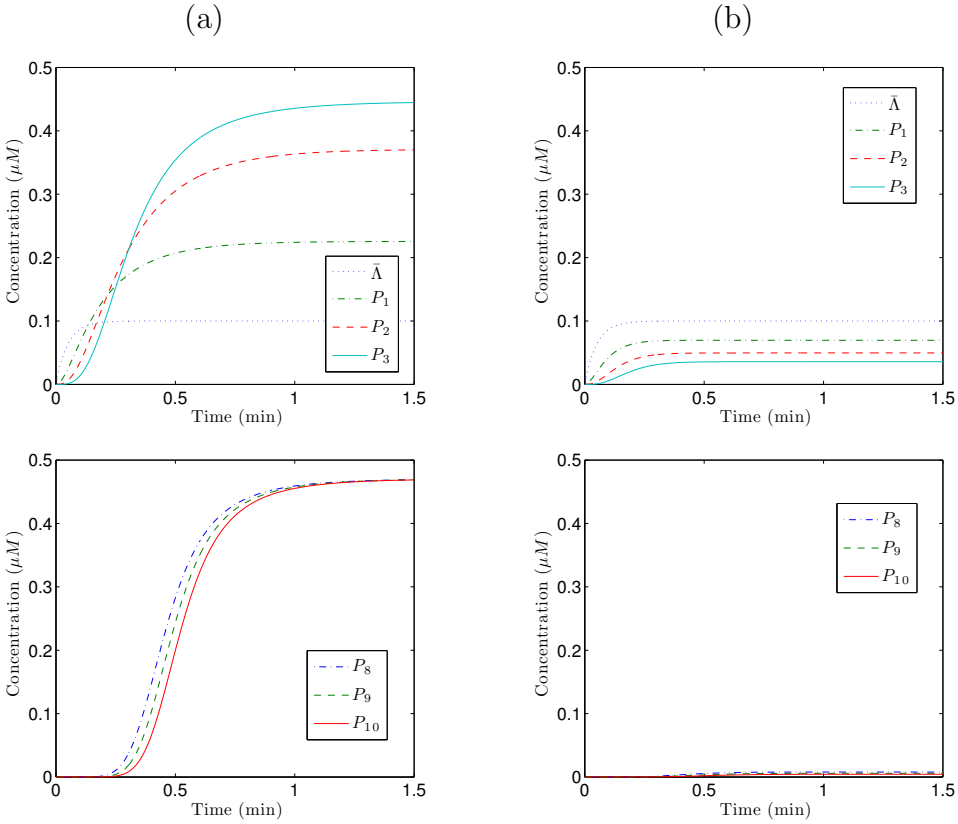

Figure 2.8: Plots of the output of an enzymatic cascade with enzyme destruction. In (a), the enzyme destruction rate is low, $\gamma\bar{S} = 3$. In (b), the enzyme destruction rate is high, $\gamma\bar{S} = 0.75$. To generate the results, Equation (2.20) was integrated with the parameters $\bar{E} = 0.1\mu M$, $\bar{S}_i = 0.5\mu M$, and $a_i = 30(\mu M\ min)^{-1}$. In column (a), $\tilde{d}_i = 5\, min^{-1}$. In column (b), $\tilde{d}_i = 20\, min^{-1}$. The input function for both columns is $\bar{\Lambda} = \bar{E}\,(1 - \exp(-\omega t))$ with $\omega = 20\ min^{-1}$.

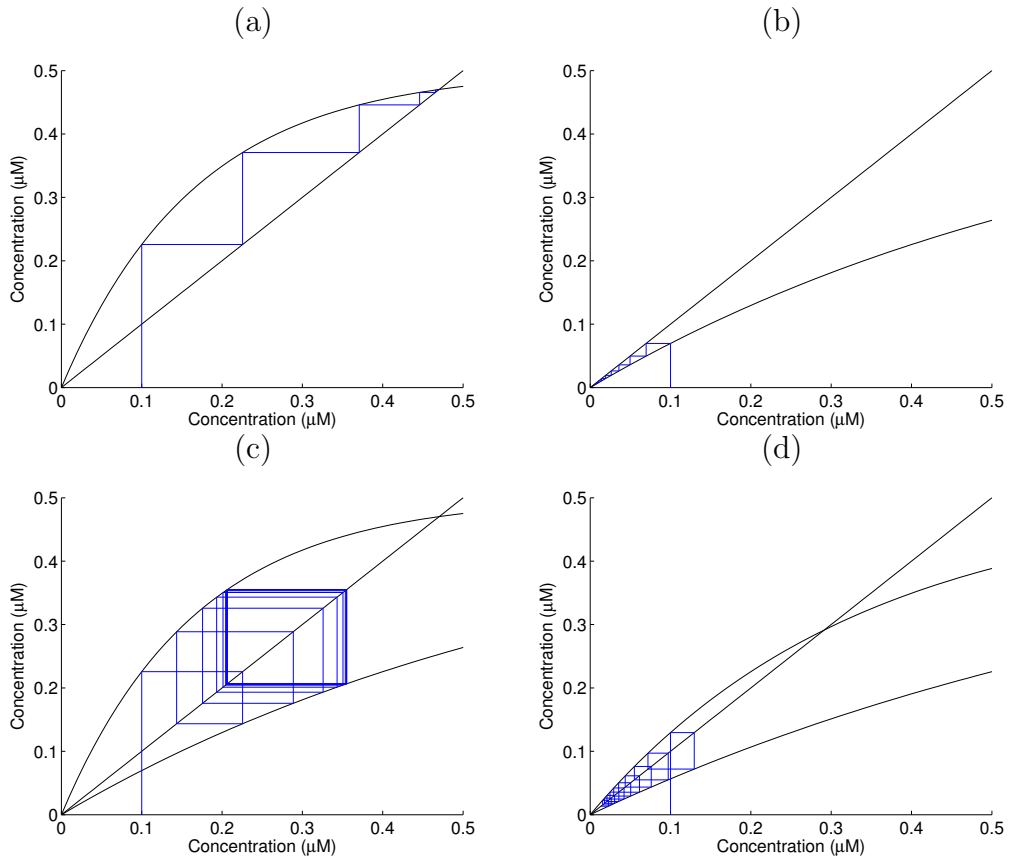

Figure 2.9: Cobweb plots of the limiting behavior of the output for an n-stage enzymatic cascade with enzyme destruction. The steady-state for an $n+1$ stage cascade is plotted against the steady-state of an n stage cascade. In (a), the enzyme destruction rate is low, $\gamma\bar{S} = 3$. In (b), the enzyme destruction rate is high, $\gamma\bar{S} = 0.75$. In (c), the module parameters alternate between $\gamma\bar{S} = 3$ and $\gamma\bar{S} = 0.75$. In (d), the module parameters alternate between $\gamma\bar{S} = 1.5$ and $\gamma\bar{S} = 0.6$.

2.4 Enzymatic Cascade with Complex Formation and Enzyme Destruction

The model seen in Figure 2.7 can be made more relevant with the addition of complex formation.

The stoichiometry looks like:

$$\begin{aligned}
\varnothing &\underset{\tilde{d}_0}{\overset{\bar{\lambda}(t)}{\rightleftarrows}} E,\\
E + S_1 &\underset{d_1}{\overset{a_1}{\rightleftarrows}} C_1 \xrightarrow{k_1} E + P_1,\\
P_1 &\xrightarrow{\tilde{d}_1} \varnothing,\\
P_1 + S_2 &\underset{d_2}{\overset{a_2}{\rightleftarrows}} C_2 \xrightarrow{k_2} P_1 + P_2,\\
P_2 &\xrightarrow{\tilde{d}_2} \varnothing,\\
&\vdots\\
P_{n-1} + S_n &\underset{d_n}{\overset{a_n}{\rightleftarrows}} C_n \xrightarrow{k_n} P_{n-1} + P_n.
\end{aligned}$$

The corresponding set of mass-action equations is:

$$\begin{aligned}
\dot{E} &= \bar{\lambda}(t) - \tilde{d}_0 E - a_1 E S_1 + (d_1 + k_1) C_1,\\
\dot{S}_1 &= -a_1 E S_1 + d_1 C_1,\\
\dot{C}_1 &= a_1 E S_1 - (d_1 + k_1) C_1,\\
\dot{P}_1 &= k_1 C_1 - \tilde{d}_1 P_1 - a_2 P_1 S_2 + (d_2 + k_2) C_2,\\
\dot{S}_2 &= -a_2 P_1 S_2 + d_2 C_2,\\
\dot{C}_2 &= a_2 P_1 S_2 - (d_2 + k_2) C_2,\\
\dot{P}_2 &= k_2 C_2 - \tilde{d}_2 P_2 - a_3 P_2 S_3 + (d_3 + k_3) C_3,\\
&\vdots\\
\dot{S}_n &= -a_n P_{n-1} S_n + d_n C_n,\\
\dot{C}_n &= a_n P_{n-1} S_n - (d_n + k_n) C_n,\\
\dot{P}_n &= k_n C_n,\\
E(0) = C_i(0) &= P_i(0) = 0, \quad S(0) = \bar{S}_i, \quad \text{for } 1 \le i \le n.
\end{aligned} \tag{2.25}$$

A module will have the form:

$$\begin{aligned}
\dot{E} &= \bar{\lambda}(t) - \tilde{d}_0 E - a_1 ES + (d_1 + k_1)C, \\
\dot{S} &= -a_1 ES + d_1 C, \\
\dot{C} &= a_1 ES - (d_1 + k_1)C, \\
\dot{P} &= k_1 C, \\
E(0) &= C(0) = P(0) = 0, \quad S(0) = \bar{S}.
\end{aligned} \tag{2.26}$$

System (2.26) can be reduced one dimension using the mass conservation equation:

$$S + C + P = \bar{S}.$$

Let

$$\begin{aligned}
S_C &= S + C, \\
E_C &= E + C.
\end{aligned}$$

Then system (2.26) is equivalent to

$$\begin{aligned}
\dot{E}_C &= \bar{\lambda}(t) - \tilde{d}_0(E_C - C), \\
\dot{S}_C &= -k_1 C, \\
\dot{C} &= a_1(E_C - C)(S_C - C) - (d_1 + k_1)C, \\
E(0) &= C(0) = 0, \quad S(0) = \bar{S}.
\end{aligned} \tag{2.27}$$

There are multiple time-scales that system (2.27) operates on. Let

$$\bar{\Lambda}(t) = \int_0^t \bar{\lambda}(x)dx,$$

and suppose that

$$\sup\{\bar{\lambda}\} = \bar{E}\omega, \quad \sup\{\bar{\Lambda}\} = \bar{E}.$$

Then the timescale that E_C operates on can be estimated by:

$$\frac{E_{Cmax} - E_{Cmin}}{\left|\dot{E}_C\right|_{max}} \approx \frac{\bar{E}}{\bar{E}\omega} = \frac{1}{\omega} := t_E.$$

The argument for the supremum of C is similar to that given in the derivation of Equation (2.12). Let

$$\tau = \frac{t}{t_E},\ \lambda_I(\tau) = \frac{\bar{\lambda}(t)}{\bar{E}\omega},\ \Lambda_I(\tau) = \frac{\bar{\Lambda}(t)}{\bar{E}},$$
$$m_I(\tau) = \frac{E_C(t)}{\bar{E}},\ s_{c_I}(\tau) = \frac{S_C(t)}{\bar{S}},\ c_I(\tau) = \frac{C(t)}{\bar{C}}.$$

A few dimensionless parameters can be defined:

$$\gamma = \frac{a_1}{\tilde{d}_0}, \quad \kappa = \frac{d_1}{k_1}, \quad \alpha_1 = \frac{\tilde{d}_0}{\omega}, \quad \alpha_2 = \frac{k_1}{\omega}, \quad \sigma = \frac{\bar{S}}{K_m}, \quad \epsilon = \frac{\bar{E}}{\bar{S} + K_m}. \tag{2.28}$$

K_m and $\bar{C}$ are defined in Equations (2.12) and (2.13). Then system (2.27) is equivalent to the scaled system:

$$\begin{aligned}
m_I'(\tau) &= \lambda_I(\tau) - \alpha_1 \left(m_I - \frac{\sigma}{\sigma + 1} c_I \right), \\
s_{c_I}' &= -\alpha_2 \epsilon c_I, \\
c_I'(\tau) &= \alpha_2(\kappa + 1) \left[((\sigma + 1)m_I - \sigma c_I)(s_{c_I} - \epsilon c_I) - c_I \right], \\
m_I(0) &= c_I(0) = 0, \quad s_{c_I}(0) = 1.
\end{aligned} \tag{2.29}$$

Suppose that $\epsilon \ll 1$ and that m_I, c_I, and s_{c_I} can be expanded in powers of ϵ as follows:

$$m_I = m_{I0} + \epsilon m_{I1} + \epsilon^2 m_{I2} + \cdots,$$
$$s_{c_I} = s_{c_{I0}} + \epsilon s_{c_{I1}} + \epsilon^2 s_{c_{I2}} + \cdots,$$
$$c_I = c_{I0} + \epsilon c_{I1} + \epsilon^2 c_{I2} + \cdots.$$

The $O(1)$ approximation of (2.29) is

$$\begin{aligned} s_{c_{I0}}(\tau) &= 1, \\ m'_{I0}(\tau) &= \lambda_I - \alpha_1 \left(m_{I0} - \frac{\sigma}{\sigma+1} c_{I0} \right), \\ c'_{I0}(\tau) &= \alpha_2(\kappa+1)(\sigma+1)(m_{I0} - c_{I0}), \\ m_{I0} &= c_{I0} = 0. \end{aligned} \tag{2.30}$$

Let $a = \frac{\sigma}{\sigma+1}$ and $b = (\sigma+1)(\kappa+1)$. Then system (2.30) can be expressed as follows:

$$\begin{bmatrix} m'_{I0}(\tau) \\ c'_{I0}(\tau) \end{bmatrix} = A \begin{bmatrix} m_{I0}(\tau) \\ c_{I0}(\tau) \end{bmatrix} + \begin{bmatrix} \lambda_I(\tau) \\ 0 \end{bmatrix}$$

where

$$A = \begin{bmatrix} -\alpha_1 & \alpha_1 a \\ \alpha_2 b & -\alpha_2 b \end{bmatrix}.$$

It can be shown that both eigenvalues of A will be real and negative. m_{I0} and c_{I0} can be solved explicitly using Variation of Parameters.

However, to capture the limiting behavior of system (2.26), it will be necessary to derive an estimate for the timescale that S_C operates on. It is difficult to estimate the timescale of S_C in general, but a similar argument to the derivation of Equation (2.14) can be used. Let

$$t_{S_C} = \frac{\bar{S} + K_m}{k_1 \bar{E}},$$

and

$$\begin{gathered} T = \frac{t}{t_{S_C}},\ \lambda_o(T) = \frac{\bar{\lambda}(t)}{\bar{E}\omega},\ \Lambda_o(T) = \frac{\bar{\Lambda}(t)}{\bar{E}}, \\ m_o(T) = \frac{E_C(t)}{\bar{E}},\ s_{c_o}(T) = \frac{S_C(t)}{\bar{S}},\ c_o(T) = \frac{C(t)}{\bar{C}}. \end{gathered}$$

Let the dimensionless parameters be defined as in Equation (2.28). Then system

(2.26) is equivalent to:

$$\begin{aligned}
\alpha_2 \epsilon m_o'(T) &= \lambda(T) - \alpha_1 \left(m_o(T) - \frac{\sigma}{\sigma+1} c_o(T) \right), \\
s_{c_o}'(T) &= -c, \\
\epsilon c_o'(T) &= (\kappa+1)\left[((\sigma+1)m_o - \sigma c_o)(s_{c_o} - \epsilon c_o) - c \right], \\
m_o(0) &= c(0) = 0, \quad s_{c_o}(0) = 1.
\end{aligned} \tag{2.31}$$

If $\epsilon \ll 1$ and m_o, s_{c_o}, and c_o can be expressed as a power series in ϵ, then the $O(1)$ approximation to system (2.31) is

$$\begin{aligned}
0 &= \lambda(T) - \alpha_1 \left((m_{o0} - \frac{\sigma}{\sigma+1} c_{o0} \right), \\
s_{c_o 0}'(T) &= -c_{o0}, \\
0 &= ((\sigma+1)m_{o0} - \sigma c_{o0}) s_{c_o 0} - c_{o0}, \\
s_{c_o 0}(0) &= 1.
\end{aligned}$$

$s_{c_o 0}$ can be solved explicitly as

$$s_{c_o 0}(T) = \exp\left(-\frac{\sigma+1}{\alpha_1} \int_0^T \lambda(x) dx \right) = \exp\left(\frac{-(\sigma+1)}{\alpha_1 t_{S_C} \omega} \Lambda(T) \right).$$

Therefore,

$$\lim_{t\to\infty} S_C(t) \approx \lim_{T\to\infty} \bar{S} s_{c_o 0}(T) = \bar{S} \exp\left(\frac{-\gamma}{\kappa+1} \bar{E} \right),$$

and

$$\bar{P} = \lim_{t\to\infty} P(t) \approx \lim_{T\to\infty} \bar{S} - \bar{S} s_{c_o 0}(T) = \bar{S} \left(1 - \exp\left(\frac{-\gamma}{\kappa+1} \bar{E} \right) \right).$$

So if all the modules are identical, then the limiting behavior of the product formation can be determined iteratively as follows:

$$\bar{P}_{n+1} = \bar{S} \left(1 - \exp\left(\frac{-\gamma}{\kappa+1} \bar{P}_n \right) \right).$$

The results from the previous section can be extended to a model with complex formation. Mainly,

Lemma 2.4.1 *Suppose a cascade is represented by system* (2.25) *with identical modules and module parameters* $\bar{S}$ *and* γ *and* κ. *If* $\bar{S}\frac{\gamma}{\kappa+1} \leq 1$, *then* $\lim_{n\to\infty} \bar{P}_n = 0$. *If* $\bar{S}\frac{\gamma}{\kappa+1} > 1$, *then there exists* $\bar{E}_{crit}$ *such that* $\bar{E}_{crit} = \bar{S}\left(1 - \exp(-\frac{\gamma}{\kappa+1}\bar{E}_{crit})\right)$ *and* $\lim_{n\to\infty} \bar{P}_n = \bar{E}_{crit}$.

The proof follows the same as the proof for Lemma 2.3.1.

2.4.1 Simulation Results and Discussion

To study the behavior of a cascade with complex formation and enzyme destruction, singular perturbation was used to approximate the system when $\bar{E}/(\bar{S} + K_m)$ is small. The approximation for the total enzyme concentration appears to work well if the time is scaled by t_E. The limiting behavior of s_c is approximated well by the $O(1)$ equations when the time is scaled by t_{S_C}, but this approximation does not appear to capture the beginning behavior of s_c. More than likely, this is the result of approximating $S_{C_{max}} - S_{C_{min}}$ as $\bar{S}$. Figure 2.10 demonstrates the results of the perturbation scheme.

Figure 2.11 demonstrates that an enzymatic cascade with complex formation and enzyme destruction behaves similarly to the simpler model without complex formation. The familiar sigmoidal shape and shift to the right appears in Column (a) where the enzyme destruction rate is low. In Column (b), the steady-state of the output diminishes with the addition of extra layers when the destruction rate is high. The relevant parameter that determines whether zero will be an attractor is $\gamma\bar{S}/(\kappa + 1)$. So the addition of complex formation will only have a detrimental effect on these types of cascades. If κ is large, then zero will have a greater chance of becoming an attractor. This makes intuitive sense since $\kappa = d_1/k_1$. If $\kappa \gg 1$, then the products are less likely to form.

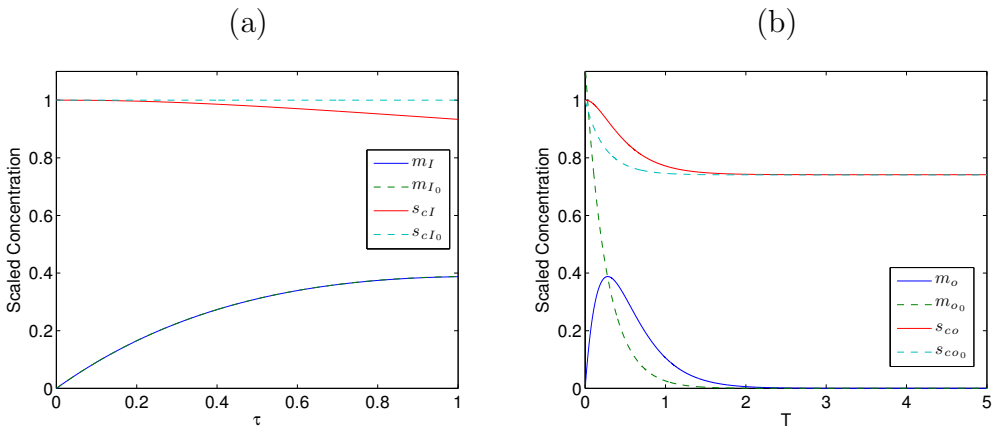

Figure 2.10: Perturbation approximation to an enzymatic cascade with complex formation and enzyme destruction. In (a), the solution on the time scale t_E is plotted. In (b), the limiting behavior of s_c can be approximated by scaling by t_{S_C}. Equations (2.29) and (2.31) were integrated using the parameters $\bar{E} = 0.1\mu M$, $\bar{S} = 0.5\mu M$, $a_1 = 30(\mu M\ min)^{-1}$, $k_1 = d_1 = 60\ min^{-1}$, and $\tilde{d}_0 = 5\ min^{-1}$. The input function is $\bar{\Lambda} = \bar{E}\,(1 - \exp(-\omega t))$ with $\omega = 5\ min^{-1}$.

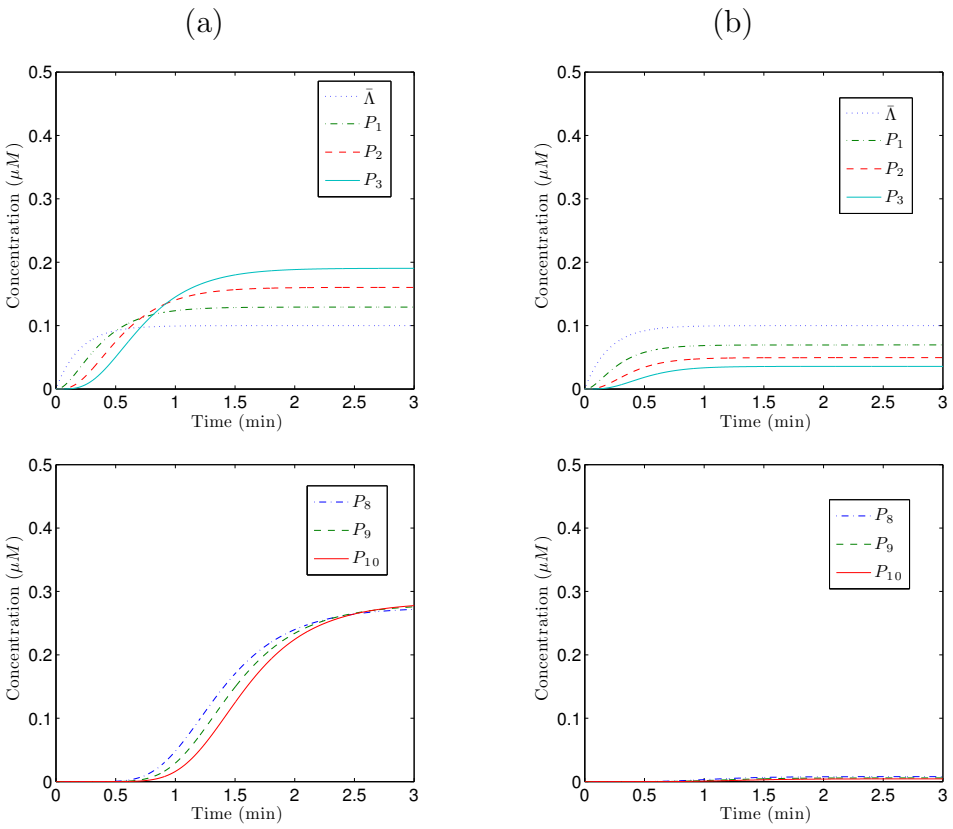

Figure 2.11: Plots of the output of an enzymatic cascade with enzyme destruction and complex formation. In column (a), the enzyme destruction rate is low. In column (b), the enzyme destruction rate is high. The same parameters used to generate Figure 2.10 were used to generate these results. However, in column (a) $\tilde{d}_i = 5 min^{-1}$, and in column (b) $\tilde{d}_i = 10\, min^{-1}$.

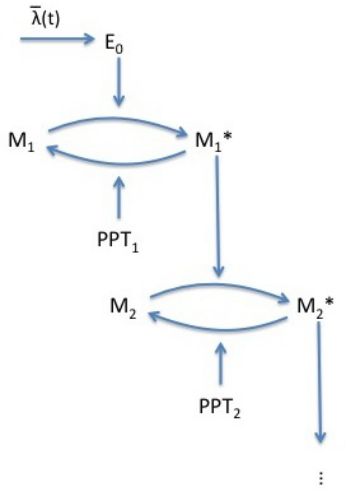

Figure 2.12: A basic signaling cascade.

In a typical signaling cascade, a phosphatase will convert a product back into a substrate, as seen in Figure 2.12. The stoichiometry governing the reactions looks like:

$$\begin{aligned}
\varnothing &\xrightarrow{\bar{\lambda}(t)} E, \\
E + M_1 &\underset{d_1}{\overset{a_1}{\rightleftarrows}} C_1 \xrightarrow{k_1} E + M_1^*, \\
PPT_1 + M_1^* &\underset{\tilde{d}_1}{\overset{\tilde{a}_1}{\rightleftarrows}} X_1 \xrightarrow{\tilde{k}_1} PPT_1 + M_1, \\
M_1^* + M_2 &\underset{d_2}{\overset{a_2}{\rightleftarrows}} C_2 \xrightarrow{k_2} M_1^* + M_2^*, \\
PPT_2 + M_2^* &\underset{\tilde{d}_2}{\overset{\tilde{a}_2}{\rightleftarrows}} X_2 \xrightarrow{\tilde{k}_2} PPT_2 + M_2, \\
&\vdots
\end{aligned}$$

where for every level i, the variables M_i, M_i^*, C_i, PPT_i, X_i denote the protein, its activated form, the intermediate complex between the kinase and the protein it acts on, the phosphatase and the intermediate complex between the phosphatase and the

protein it acts on, respectively. The corresponding set of mass-action equations is:

$$
\begin{aligned}
\dot{E} &= \bar{\lambda}(t) - a_1 E M_1 + (d_1 + k_1) C_1, \\
\dot{M}_1 &= -a_1 E M_1 + d_1 C_1 + \tilde{k}_1 X_1, \\
\dot{C}_1 &= a_1 E M_1 - (d_1 + k_1) C_1, \\
\dot{M}_1^* &= k_1 C_1 - \tilde{a}_1 P P T_1 M_1^* + \tilde{d}_1 X_1 - a_2 M_1^* M_2 + (d_2 + k_2) C_2, \\
P\dot{P}T_1 &= -\tilde{a}_1 P P T_1 M_1^* + (\tilde{d}_1 + \tilde{k}_1) X_1, \\
\dot{X}_1 &= \tilde{a}_1 P P T_1 M_1^* - (\tilde{d}_1 + \tilde{k}_1) X_1, \\
&\vdots \\
\dot{M}_n &= -a_n M_n^* M_n + d_n C_n + \tilde{k}_n X_n, \\
\dot{C}_n &= a_n M_n^* M_n - (d_n + k_n) C_n, \\
\dot{M}_n^* &= k_n C_n - \tilde{a}_n P P T_n M_n^* + \tilde{d}_n X_n \\
P\dot{P}T_n &= -\tilde{a}_n P P T_n M_n^* + (\tilde{d}_n + \tilde{k}_n) X_n, \\
\dot{X}_n &= \tilde{a}_n P P T_n M_n^* - (\tilde{d}_n + \tilde{k}_n) X_n, \\
E(0) &= M_i^*(0) = C_i(0) = X_i(0) = 0, \\
M_i(0) &= \bar{M}_i, \text{ and } PPT_i(0) = \overline{PPT}_i \text{ for } 1 \leq i \leq n.
\end{aligned}
\tag{2.32}
$$

2.5.1 Simulation Results and Discussion

Figure 2.13 demonstrates that the signaling cascade can convert many different types of input signals into a smooth, sigmoidal output. The addition of extra layers can decrease the activation time up to a point, after which the addition of more layers will only cause a delay. With identical modules, the number of layers needed to reach an optimal activation time depends on the rate that the input signal is coming in. Some previous studies have examined the noise-filtering properties of signaling cascades [24, 33]. A previous paper looked at the noise-filtering characteristics of a simple

module of a protein with opposing covalent modifications. The parameters used to generate Figure 2.13 were taken from the range listed in [23]. Since the behavior of the signaling cascade is also observed in the most basic model, this strongly suggests that the cascade architecture is also responsible for the noise-filtering properties.

Figure 2.14 shows what happens when the phosphatase concentration is too high. Each additional layer will only cause the steady-state value of the output to diminish. This behavior was also observed in a basic model with enzyme destruction. It may be possible to derive an iterative map for the steady-state values. Figure 2.15 shows another interesting property of multi-layered signaling cascades. If the phosphatase concentration is low, than each additional layer will extend the time that the proteins remain in an active state in response to a brief pulse. If the phosphatase concentration is too high, then a brief pulse will not elicit a response.

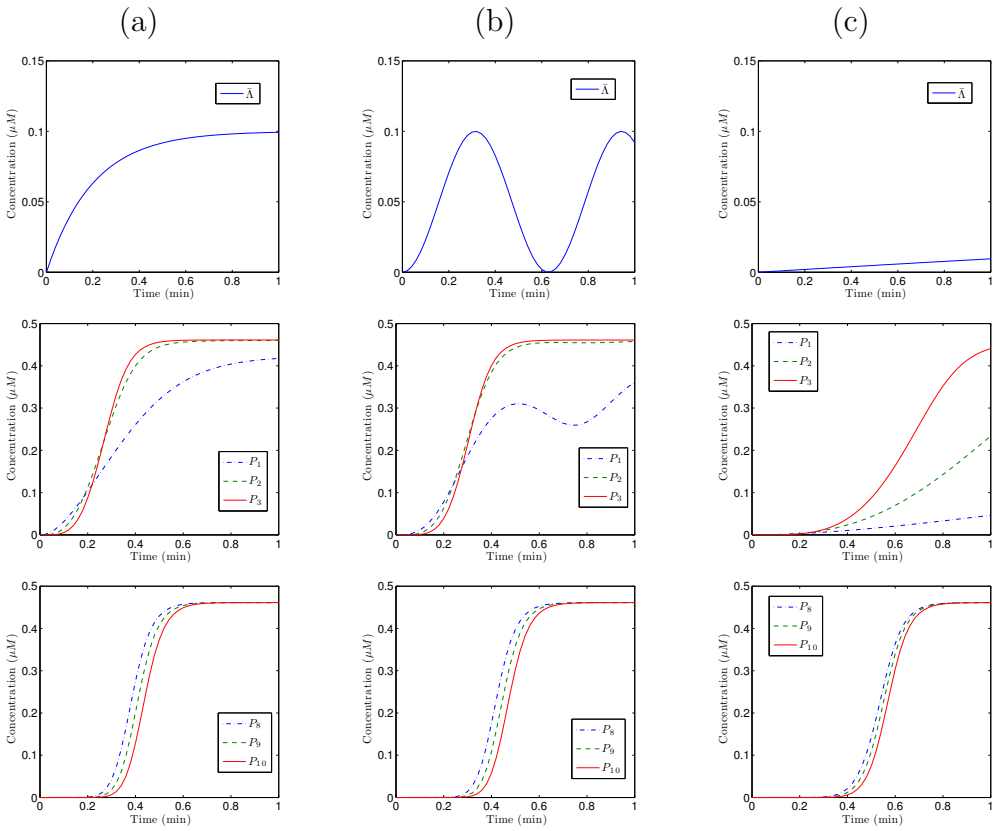

Figure 2.13: Plots of various inputs and their outputs for a basic signaling cascade with identical modules. In the first row, various input signals are plotted. In column (a), $\bar{\Lambda} = \bar{E}\left(1 - \exp(-\omega t)\right)$ with $\omega = 5\ min^{-1}$. In column (b), $\bar{\Lambda} = \bar{E}\left(1 - \cos(\omega t)\right)/2$ with $\omega = 10\ min^{-1}$. In column (c), $\bar{\Lambda} = \bar{E}\left(1 - \exp(-\omega t)\right)$ with $\omega = 0.1\ min^{-1}$. Equation (2.32) was integrated for the various inputs with $\bar{E} = 0.1\mu M$, $\bar{S}_i = 0.5\mu M$, $\overline{PPT}_i = 0.024\mu M$, $a_i = 200(\mu M\ min)^{-1}$, and $k_i = d_i = 30\ min^{-1}$. The second row shows that various inputs have a sigmoidal output after three layers and that the activation time moves to the left. The last row shows what an 8, 9, and 10 layer cascade would do to the input. Eventually, the activation time moves to the right. The results are very similar to the results for a basic cascade without complex formation.

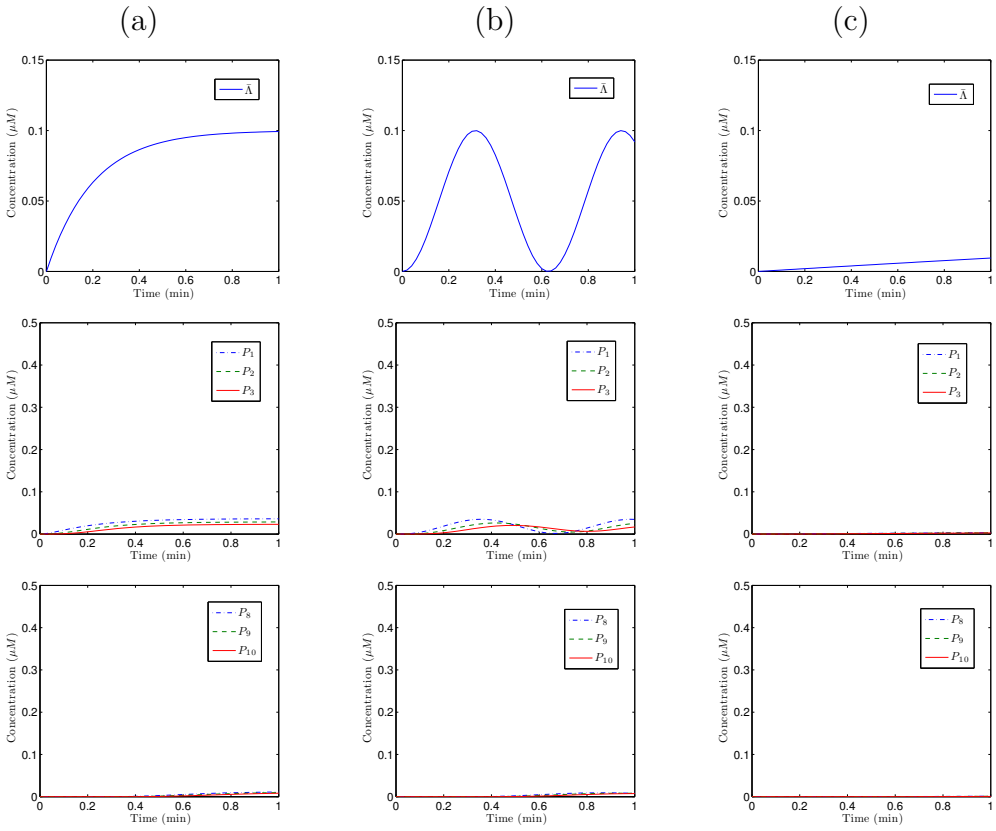

Figure 2.14: Plots of various inputs and their outputs for a basic signaling cascade with identical modules. In the first row, various input signals are plotted. In column (a), $\bar{\Lambda} = \bar{E}\left(1 - \exp(-\omega t)\right)$ with $\omega = 5\ min^{-1}$. In column (b), $\bar{\Lambda} = \bar{E}\left(1 - \cos(\omega t)\right)/2$ with $\omega = 10\ min^{-1}$. In column (c), $\bar{\Lambda} = \bar{E}\left(1 - \exp(-\omega t)\right)$ with $\omega = 0.1\ min^{-1}$. Equation (2.32) was integrated for the various inputs with $\bar{E} = 0.1\mu M$, $\bar{S}_i = 0.5\mu M$, $\overline{PPT}_i = 0.5\mu M$, $a_i = 200(\mu M\, min)^{-1}$, and $k_i = d_i = 30 min^{-1}$. The results show that a high phosphatase concentration can prevent the output from activating. The results are similar to the results for a basic enzymatic cascade with enzyme destruction and a high destruction rate.

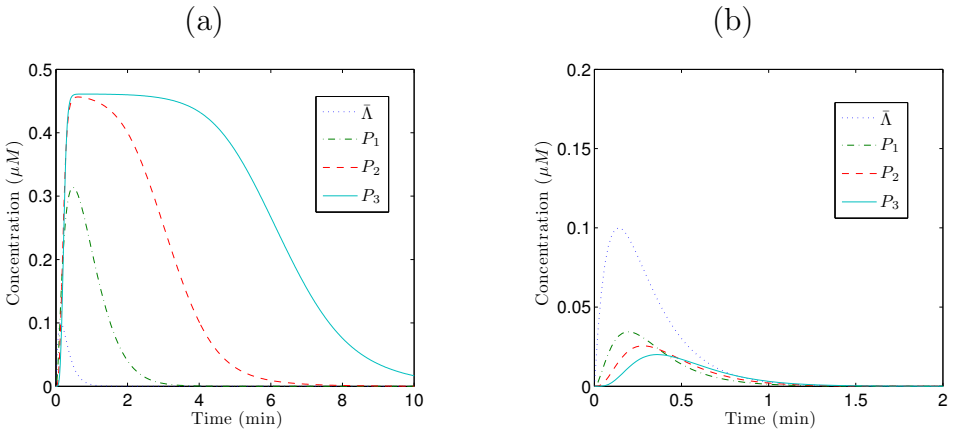

Figure 2.15: Plots of the output with a pulse input. In (a), the phosphatase concentration is an order lower than the substrate concentration. In (b), the phosphatase concentration is the same as the substrate concentration. The same parameters used to generate Figure 2.14 were used to generate these results. However, the input function is $\bar{\Lambda} = \bar{E}\,(1 - \exp(-\omega t))\exp(-\omega t)$ with $\omega = 5\ min^{-1}$.

Chapter 3

CONCLUSION AND FUTURE OUTLOOK

Much work has been done over the years in analyzing mass-action models of enzymatic reactions. Numerous studies have been made that examined the Michaelis-Menten approximation of closed enzymatic systems, and some studies have been made towards analyzing perturbation approximations of open-enzymatic reactions; however, this is the first work to rigorously show that Michaelis-Menten parameters derived from closed experiments are applicable to open-enzymatic systems under certain conditions. It was argued in [34] that many researchers use the Michaelis-Menten approximation without first validating the conditions under which the approximation is valid. One such situation that has not been looked at in detail is the use of the Michaelis-Menten approximation for enzyme-substrate reactions when those reactions are embedded in larger chemical networks. This will be a major boon to systems biologists since most parameters for enzymatic reactions are derived from isolated experiments, but since these parameters are available in the literature, they are used in networked modules.

This work validated the approximation when $\epsilon = \bar{E}/(\bar{S}+K_m) \ll 1$ and for systems with an influx of enzymes. More work can be done to see what happens when $\epsilon = O(1)$ or when $\epsilon \gg 1$. Models with feedback, an influx of substrate, and a combination of other tweaks, can also be examined in the future.

This research also highlighted the issue of error accumulation, but more work needs to be done to examine how errors will propagate and accumulate through a complicated network of chemical reactions. This is an interesting problem, but it is not immediately obvious whether doing a parameter sensitivity analysis and error

analysis on individual modules will be useful in general models. Studying a chain of simple modules is a starting point, but more complicated networks may need a different approach.

As stated in [19], MAPK cascades typically have three or four layers. The benefits of a multi-stage cascade have been studied before, but this work is the first to rigorously examine the time-dependent properties of the cascade architecture. Previous authors have looked at the noise-filtering characteristics of signaling cascades, but this is the first work to argue that the noise-filtering is inherent in the basic cascade architecture, regardless of whether the modules have an opposing covalently modified protein. Three stages are needed to filter out noise and transmit the relevant information downstream, and too many identical layers may actually cause a delay in the activation time, which suggests an evolutionary benefit to limiting the number of tiers of a cascade to just a few. The basic versions of the cascades exhibit these same behaviors as do their more complicated counterparts.

As stated in [35], the phosphatase concentrations in signaling cascades are relatively small compared to the other constituent reactants. If the phosphatase concentration is low, signaling cascades will behave similarly to a basic enzymatic cascade without complex formation. This involved iterating functions of the type:

$$1 - \exp\left(-\int_0^T \Lambda(x)dx\right).$$

Though several properties of the function operator were proven, there is still an interesting, open conjecture about whether signals from Λ_{set} will turn sigmoidal eventually. Given the properties of Λ_{set}, the operator involves iterating functions that define distribution functions, so tools from probability theory can be employed to answer the question.

High phosphatase concentrations can be detrimental to the output of signaling

cascades. By examining a simple cascade with enzyme destruction, it was shown that if the phosphatase concentration is too high relative to the other constituent reactants, then the steady-state value of the output will drop with each additional layer of the cascade; zero becomes an attracting fixed point. This behavior was also seen in more complicated models. A high phosphatase concentration can also destroy another dynamical property of signaling cascades, the ability to sustain a signal after a brief input. More work needs to be done to examine precisely why the cascade architecture will sustain a signal in such a way. It is believed that the framework of examining simple modules will be a fruitful avenue.

An interesting future research project would be to verify experimentally the properties observed in the iterative models of signaling cascades. A more comprehensive study of the rate parameters seen in signaling cascades can be undertaken. The filtering properties are dependent on the phosphatase concentrations, and the increase or delay of the activation time is dependent on the model parameters. It would be interesting to see if actual cascades are tuned to compensate for these effects. It would be beneficial to collaborate with wet-lab researchers in the future.

REFERENCES

[1] J. A. McCubrey and *et al*. Roles of the raf/mek/erk pathway in cell growth, malignant transformation and drug resistance. *Biochimica et Biophysica Acta*, 1773:1263–1284, 2007.

[2] D. Marx and J. Hutter. *Ab Initio Molecular Dynamics*. Cambridge University Press Textbooks, 2009.

[3] D. Higham. Modeling and simulating chemical reactions. *SIAM Review*, 50(2):347–368, 2008.

[4] D. T. Gillespie. A general method for numerically simulating the stochastic time evolution of coupled chemical reactions. *Journal of Computational Physics*, 22(4):403–434, 1976.

[5] D. T. Gillespie. Exact stochastic simulation of coupled chemical reactions. *Journal of Physical Chemistry*, 81(25):2340–2361, 1977.

[6] M.A. Gibson and J. Bruck. Efficient exact stochastic simulation of chemical systems with many species and many channels. *Journal of Physical Chemistry A*, 104(9):1876–1889, 2000.

[7] D. T. Gillespie. Approximate accelerated stochastic simulation of chemically reacting systems. *The Journal of Chemical Physics*, 115(4):1716–1733, 2001.

[8] D. T. Gillespie. The chemical langevin equation. *Journal of Chemical Physics*, 113:297–306, 2000.

[9] S. Schnell and T.E. Turner. Reaction kinetics in intracellular environments with macromolecular crowding: simulations and rate laws. *Progress in Biophysics and Molecular Biology*, 85:235–260, 2004.

[10] D. J. Wilkinson. *Stochastic Modelling for Systems Biology*. Chapman & Hall/CRC, 2006.

[11] L. Michaelis and M. L. Menten. Die kinetik der invertinwirkung. *Biochemische Zeitschrift*, 49:333–369, 1913.

[12] K. A. Johnson and R. S. Goody. The original michaelis constant: Translation of the 1913 michaelis-menten paper. *Biochemistry*, 50(39):8264–8269, 2011.

[13] G. E. Briggs and J.B.S Haldane. A note on the kinetics of enzyme action. *Biochemical Journal*, pages 338–339, 1925.

[14] S. Schell and C. Mendoza. A closed-form solution for time-dependent enzyme kinetics. *Journal of Theoretical Biology*, 187:207–212, 1997.

[15] R. M. Corless and *et al*. On the lambertw function. *Advances in Computational Mathematics*, 5(1):329–359, 1996.

[16] E. W. Davie and O. D. Ratnoff. Waterfall sequence for intrinsic blood clotting. *Science*, 145(3638):1310–1312, September 1964.

[17] R. G. Macfarlane. An enzyme cascade in the blood clotting mechanism, and its function as a biochemical amplifier. *Nature*, 202:498–499, 1964.

[18] S. N. Levine. Enzyme amplifier kinetics. *Science*, 152(3722):651–653, April 1966.

[19] E. Klipp and *et al*. *Systems Biology*. Wiley-VCH Verlg GmbH & Co. KGaA, Weinheim, 2009.

[20] W. Kolch. Meaningful relationships: The regulation of the RAS/Raf/MEK/ERK pathway by protein interactions. *Biochemical Journal*, 351:289–305, 2000.

[21] C.Y. Huang and J.E. Ferrell. Ultrasensitivity in the mitogen-activated protein kinase cascade. *Proceedings of the National Academy of Sciences*, 93:10078–10083, September 1996.

[22] A. Goldbeter and D. E. Koshland. Ultrasensitivity in biochemical systems controlled by covalent modification: Interplay between zero-order and multistep effects. *Journal of Biological Chemistry*, 259:14441–14447, 1984.

[23] L. Qiao and *et al*. Bistability and oscillations in the huang-ferrell model of mapk signaling. *PLoS Computational Biology*, 3(9):1819–1826, 2007.

[24] C. Gomez-Uribe and *et al*. Operating regimes of signaling cycles: Statics, dynamics, and noise filtering. *PLoS Computational Biology*, 3(12):2487–2497, 2007.

[25] J. Borghans and *et al*. Extending the quasi-steady state approximation by changing variables. *Bulletin of Mathematical Biology*, 58:43–63, 1996.

[26] M. H. Holmes. *Introduction to Perturbation Methods*. Springer Verlag New York, Inc., 1995.

[27] C. C. Lin and L. A. Segel. *Mathematics Applied to Deterministic Problems in Natural Sciences*. Macmillan Publishing, 1974.

[28] F.G. Heineken, H.M. Tsuchiya, and R. Aris. On the mathematical status of the pseudo-steady state hypothesis of biochemical kinetics. *Mathematical Biosciences*, 1(1):95 – 113, 1967.

[29] L. A. Segel and M. Slemrod. The quasi-steady-state assumption: A case study in perturbation. *SIAM Review*, 31(3):446–447, 1989.

[30] M. Bagnoli and T. Bergstrom. Log-concave probability and its applications. In C. D. Aliprantis and *et al*, editors, *Rationality and Equilibrium*, volume 26 of *Studies in Economic Theory*, pages 217–241. Springer Berlin Heidelberg, 2006.

[31] P. L. Brockett and J. H. B. Kemperman. On the unimodality of high convolutions. *Annals of Probability*, 10(1):270–277, 1982.

[32] M. W. Hirsch and S. Smale R. L. Devaney. *Differential Equations, Dynamical Systems, and an Introduction to Chaos, 2nd Edition*. Academic Press, 2004.

[33] K. A. Fujita and *et al*. Decoupling of receptors and downstream signals in the akt pathway by its low-pass filter characteristics. *Science Signaling*, 3(132), July 2010.

[34] A. M. Bersani and G. Dell'Acqua. Is there anything left to say on enzyme kinetic constants and quasi-steady state approximation? *Journal of Mathematical Chemistry*, 50:335–344, 2012.

[35] A.C. Ventura, J-A. Sepulchre, and S.D. Merjver. A hidden feedback in signaling cascades is revealed. *PLoS Computational Biology*, 4(3):1–14, 2007.